Deletion of CTLA-4 on regulatory T cells during adulthood leads to resistance to autoimmunity

Alison M. Paterson[1,2,*], Scott B. Lovitch[1,2,3,*], Peter T. Sage[1,2], Youjin Lee[2], Carolina V. Arancibia-Cárcamo[4], Raymond A. Sobel[5], Alexander Y. Rudensky[6], Vijay K. Kuchroo[2], Gordon J. Freeman[7] and Arlene H. Sharpe[1,2,†]

[1]Department of Microbiology and Immunobiology, Harvard Medical School, [2]Evergrande Center for Immunologic Diseases, Harvard Medical School and Brigham and Women's Hospital, and [3]Department of Pathology, Brigham and Women's Hospital, Boston, MA 02115

[4]Translational Gastroenterology Unit, Nuffield Department of Clinical Medicine, Experimental Medicine Division, University of Oxford, Oxford OX3 9DU, UK

[5]Department of Pathology, Stanford University, Stanford, CA 94304

[6]Howard Hughes Medical Institute and Immunology Program, Sloan-Kettering Institute for Cancer Research; Ludwig Center at Memorial Sloan-Kettering Cancer Center, New York, NY 10065

[7]Department of Medical Oncology, Dana-Farber Cancer Institute, Boston, MA 02115

[*]These authors contributed equally to this work and share primary authorship.

[†]To whom correspondence should be addressed: arlene_sharpe@hms.harvard.edu

Running Title: CTLA-4 deletion on Treg prevents autoimmunity

Total characters: 27,280

Abstract

Cytotoxic T lymphocyte antigen-4 (CTLA-4) is an essential negative regulator of T cell responses. However, investigation of the function of CTLA-4 on mature T cells has been challenging, since mice with germline CTLA-4 deficiency develop lethal inflammation early in life. To elucidate the function of CTLA-4 on mature T cells, we have examined the function of CTLA-4 using conditional ablation in adult mice. Here, we show that in contrast to germline knockout mice, deletion of CTLA-4 during adulthood does not precipitate systemic autoimmunity, but surprisingly confers protection from experimental autoimmune encephalomyelitis (EAE), a model of multiple sclerosis. Protection from disease was accompanied by activation and expansion of both conventional $CD4^+$ $Foxp3^-$ (Tconv) and regulatory $Foxp3^+$ (Treg) T cell subsets; however, deletion of CTLA-4 on Treg was necessary and sufficient for protection. CTLA-4 deleted Treg remained functionally suppressive and induced profound changes in the CTLA-4 sufficient Tconv compartment, characterized by upregulation of immunoinhibitory molecules including IL-10, LAG-3 and PD-1, which mirror the changes seen with global CTLA-4 deletion. Taken together, our findings point to a profound role for CTLA-4 on Treg in limiting their peripheral expansion and activation, thereby shaping the phenotype and function of Tconv.

Introduction

While the specificity of T cell activation is determined by the interaction of antigenic peptide-MHC complex and the T cell receptor (TCR), the functional outcome of the T cell response is profoundly influenced by costimulatory and coinhibitory signals. The coinhibitory receptor CTLA-4 (cytotoxic T lymphocyte antigen-4; CD152) is a potent negative regulator of T cell responses (Fife and Bluestone, 2008; Sharpe and Freeman, 2002). CTLA-4 is a structural homolog of the costimulatory receptor CD28, and binds with high affinity to the same ligands, B7-1 (CD80) and B7-2 (CD86), which are primarily expressed by antigen-presenting cells (APC) (Freeman et al., 1993; Freeman et al., 1991; Harper et al., 1991; Linsley et al., 1991). However, while CD28 is constitutively expressed on most T cells, CTLA-4 is constitutively expressed only on $CD4^+Foxp3^+$ regulatory T cells (Treg) (Metzler et al., 1999; Read et al., 2000; Takahashi et al., 2000), and appears on $CD4^+Foxp3^-$ conventional T cells (Tconv) following activation (Freeman et al., 1992; Linsley et al., 1992; Walunas et al., 1996). Germline CTLA-4 deficient mice develop marked lymphocyte proliferation, resulting in splenomegaly, lymphadenopathy, myocarditis, pancreatitis, hepatitis, lung inflammation, and death within the first month of life (Tivol et al., 1995; Waterhouse et al., 1995). CTLA-4 has been implicated as a susceptibility gene in human autoimmune diseases, with several disease-associated polymorphisms reported (Gough et al., 2005; Scalapino and Daikh, 2008; Ueda et al., 2003). Furthermore, anti-CTLA-4 antibodies have demonstrated efficacy in enhancing antitumor immune responses in cancer patients (Hodi et al., 2010; Robert et al., 2011), and the anti-CTLA-4 monoclonal antibody ipilimumab is now approved by the U.S. Food and Drug Administration (FDA) as an anti-tumor therapy.

Despite the striking phenotype of the CTLA-4 deficient mouse, the mechanisms by which CTLA-4 restrains T cell activation remain controversial. Initial studies pointed to a cell-intrinsic role; a tyrosine-containing motif in the cytoplasmic tail of CTLA-4 is responsible for recruitment of phosphatases SHP-2 and PP2A, which leads to inhibition of signaling downstream of TCR (Chuang et al., 2000; Chuang et al., 1999; Cilio et al., 1998; Lee et al., 1998; Marengere et al., 1996). In addition, CTLA-4 signaling, as well as exclusion of CD28 from the immunological synapse due to preferential binding of CTLA-4 to B7 molecules, results in less activation of NF-kB, NFAT and AP-1, and inhibition of proliferation and IL-2 secretion (Fraser et al., 1999; Greenwald et al., 2002; Krummel and Allison, 1996; Olsson et al., 1999). The cytoplasmic domain of CTLA-4 is also necessary for impaired TCR signaling in Treg (Tai et al., 2012), and CTLA-4-mediated recruitment of PKC-η to the immunological synapse in Treg leads to inhibitory signaling through the PIX-GIT2-PAK2 complex (Kong et al., 2014).

While a number of studies support cell-intrinsic mechanisms of CTLA-4 function (Ise et al., 2010; Jain et al., 2010), there are also data supporting cell-extrinsic mechanisms of CTLA-4 function. Mixed bone marrow (BM) chimeras made using wild type and CTLA-4 deficient BM are healthy, whereas chimeras reconstituted with CTLA-4-deficient BM stem cells alone develop a fatal autoimmune phenotype similar to that of germline CTLA-4 deficient mice (Bachmann et al., 1999), suggesting a cell-extrinsic (i.e., *trans*-acting) function for CTLA-4 in immunoregulation.

Cell-extrinsic mechanisms of CTLA-4 function are most likely achieved by interactions of a CTLA-4-expressing cell with a B7-expressing cell. CTLA-4 has been suggested to down-regulate B7-1 or B7-2 on APC, either by indirect suppression of the

APC, signaling through B7, or direct trans-endocytosis of B7 (Fallarino et al., 2003; Onishi et al., 2008; Qureshi et al., 2011; Wing et al., 2008). Foxp3$^+$ Treg are known to act via a dominant, *trans*-acting function, and the *Ctla4* gene is a transcriptional target of Foxp3 (Wu et al., 2006; Zheng et al., 2007). Mice specifically lacking CTLA-4 on Treg (throughout development) die of an autoimmune syndrome similar to that seen in CTLA-4 deficient mice, albeit with delayed kinetics (Wing et al., 2008). In addition, the health of mixed blastocyst and bone marrow chimeras has been shown to depend on the ongoing presence of CTLA-4-sufficient Foxp3$^+$ Treg (Friedline et al., 2009).

Treg are present (in fact, expanded) in CTLA-4-deficient mice, suggesting that this molecule is not required for Treg differentiation (Schmidt et al., 2009; Tang et al., 2004). However, there is substantial support for the concept that CTLA-4 is essential for Treg suppressive function, despite ongoing controversy (reviewed in Walker, 2013). Multiple studies of antibody-mediated CTLA-4 blockade suggest a role for CTLA-4 in Treg suppressor function (Liu et al., 2001; Read et al., 2006; Read et al., 2000; Takahashi et al., 2000). However, CTLA-4-deficient Treg are capable of suppressing disease in colitis and EAE models (Read et al., 2006; Verhagen et al., 2009), although not in an adoptive transfer model of diabetes (Schmidt et al., 2009).

The role of CTLA-4 in thymic development has also been controversial. Some studies have not revealed a role (Chambers et al., 1997; Schmidt et al., 2009), while others have shown that CTLA-4 plays a role in negative selection (Buhlmann et al., 2003; Cilio et al., 1998; Takahashi et al., 2005; Wagner et al., 1996), modulating the TCR repertoire and inhibiting natural Treg generation (Verhagen et al., 2009; Verhagen et al., 2013). CTLA-4 likely opposes the critical role for CD28 in promoting negative

selection and thymic Treg differentiation (Punt et al., 1997; Punt et al., 1994; Salomon et al., 2000; Tai et al., 2005; Tang et al., 2003). The lack of a murine model in which CTLA-4 can be deleted on mature T cells in adult mice has led to ambiguity on the role of CTLA-4 in Treg function, and more generally in peripheral tolerance.

To dissect the function of CTLA-4 during adulthood, we have developed a model system in which conditional ablation of *Ctla4* can be pharmacologically induced by tamoxifen administration. Using this approach, we demonstrate that adult mice lacking CTLA-4 not only fail to develop spontaneous autoimmunity, but are also protected from development of experimental autoimmune encephalomyelitis (EAE). Protection from EAE is accompanied by marked expansion of functional Treg. Inducible deletion of CTLA-4 only on Treg in adult mice recapitulates both EAE protection and its underlying cellular phenotypes, indicating that loss of CTLA-4 function on Treg is responsible for protection from disease. Studies of gene expression show upregulation of an immunosuppressive gene expression profile in CTLA-4-deficient Treg and Tconv. Thus, CTLA-4 is not absolutely required for suppressive function of Treg, but, rather, has a Treg-intrinsic role in limiting peripheral Treg expansion and activation, and in altering their capacity to control Tconv.

Results

Deletion of *Ctla4* during adulthood does not cause autoimmunity

Due to the limitations in using the germline *Ctla4* knockout mouse to study CTLA-4 function, we generated a novel C57BL/6 strain harboring a conditional *Ctla4* allele (Fig. S1). To validate this mouse strain, we crossed $Ctla4^{fl/fl}$ to Lck^{Cre+} mice to generate $Lck^{Cre+}Ctla4^{fl/fl}$ mice, which would delete *Ctla4* in T cells expressing *Lck* during thymic selection. These mice displayed a very similar phenotype to germline Ctla4 knockout mice, developing massive lymphadenopathy and dying by 28 days of age (data not shown).

In order to study the role of CTLA-4 during adulthood, we crossed the $Ctla4^{fl/fl}$ strain to a tamoxifen-inducible Cre recombinase-expressing strain, $UBC^{Cre/ERT2}$. The resulting $UBC^{Cre/ERT2+}Ctla4^{fl/fl}$ mice were treated with tamoxifen daily for five consecutive days beginning at seven weeks of age. Within seven days of initial administration of tamoxifen, CTLA-4 mRNA expression in splenocytes from $UBC^{Cre/ERT2+}Ctla4^{fl/fl}$ mice was substantially reduced compared to $UBC^{Cre/ERT2-}Ctla4^{fl/fl}$ controls as assessed by quantitative RT-PCR (Fig. S2). Deletion of CTLA-4 at the protein level was measured by co-staining with antibodies against Foxp3 and CTLA-4 eleven days after initiation of tamoxifen treatment. Splenic $Foxp3^{+}$ regulatory T cells (Treg), which are normally 91.24±2.09% positive for CTLA-4 in $UBC^{Cre/ERT2-}Ctla4^{fl/fl}$ mice were reduced to 7.00±3.34% positive in $UBC^{Cre/ERT2+}Ctla4^{fl/fl}$ mice (Fig. 1A). While $Foxp3^{-}$ conventional T cell (Tconv) populations normally express lower levels of CTLA-4 than Treg, a reduction in CTLA-4 staining on this population was also observed. Deletion on this non-Treg subset was confirmed by staining cells after *in vitro* stimulation with anti-CD3 (data not

shown). We monitored tamoxifen-treated mice over a period of six months and no overt disease was observed in *UBC*$^{Cre/ERT2+}$*Ctla4*$^{fl/fl}$ mice when compared with *UBC*$^{Cre/ERT2-}$*Ctla4*$^{fl/fl}$ littermates or vehicle-treated controls; histological analysis of several tissues of these mice revealed no abnormalities (Fig. S3). Thus, profound, inducible deletion of *Ctla4* in adult mice does not result in a spontaneous lethal inflammation phenotype in contrast to germline *Ctla4* knockout mice.

Deletion of *Ctla4* in adult mice induces resistance to EAE

Since adult *UBC*$^{Cre/ERT2+}$*Ctla4*$^{fl/fl}$ mice treated with tamoxifen are healthy, we investigated the consequences of inducing autoimmunity in this strain by immunization with the self-peptide MOG_{35-55} to induce EAE. In contrast to *UBC*$^{Cre/ERT2-}$*Ctla4*$^{fl/fl}$ littermate controls, which developed disease, *UBC*$^{Cre/ERT2+}$*Ctla4*$^{fl/fl}$ mice were markedly resistant to EAE (Fig. 1B and Table I). Consistent with clinical disease score, *UBC*$^{Cre/ERT2+}$*Ctla4*$^{fl/fl}$ mice had fewer inflammatory foci in the brains and spinal cords than their littermate controls (Fig. S4 and Table I).

We next compared the phenotype of T cells in the cervical lymph nodes (cLN; draining the central nervous system) of control and *UBC*$^{Cre/ERT2+}$*Ctla4*$^{fl/fl}$ mice 14 days after immunization with MOG_{35-55}. Within the $CD4^+$ T cell subset, both $Foxp3^+$ Treg and $Foxp3^-$ Tconv cells were expanded in *UBC*$^{Cre/ERT2+}$*Ctla4*$^{fl/fl}$ mice when compared to *UBC*$^{Cre/ERT2-}$*Ctla4*$^{fl/fl}$ mice, with the proportional increase of Treg being greater (Fig. 2A, B). In addition, intracellular Ki-67 staining was increased in both subsets, suggesting increased peripheral expansion of these cells (Fig. 2C). Analysis of CD62L and CD44 surface staining revealed Tconv, and to a lesser extent Treg, from the

UBC$^{Cre/ERT2+}$*Ctla4*$^{fl/fl}$ mice to be more activated than those from control mice (Fig. 2D). These differences were also observed in the spleen and inguinal lymph node (draining the site of immunization) and observed prior to immunization (by 8 days after initial administration of tamoxifen; Fig. 1A and data not shown). In the central nervous system (CNS), at the onset of disease, we found a similar frequency of total CD4$^+$ T cells in both groups (data not shown), and an increase in the frequency of Treg in *UBC*$^{Cre/ERT2+}$*Ctla4*$^{fl/fl}$ mice (Fig. 2E) similar to that observed in the periphery. Treg in the CNS of UBC$^{Cre/ERT2+}$Ctla4$^{fl/fl}$ mice were profoundly deleted for CTLA-4, as in the periphery. Thus, deletion of CTLA-4 in adult mice and resistance to autoimmunity is characterized by expansion and increased activation of Tconv, but a proportionally greater expansion of Treg both in the periphery and in the target tissue.

Resistance to autoimmunity is dependent on CTLA-4 deletion on Treg

In order to determine if resistance to EAE is caused by the absence of *Ctla4* during thymic selection, we adoptively transferred mature CD4$^+$ T cells from either *UBC*$^{Cre/ERT2-}$*Ctla4*$^{fl/fl}$ or *UBC*$^{Cre/ERT2+}$*Ctla4*$^{fl/fl}$ mice into *TCR*$\alpha^{-/-}$ recipients, which were then treated with tamoxifen and immunized with MOG$_{35-55}$ to induce EAE. Recipients of *UBC*$^{Cre/ERT2+}$*Ctla4*$^{fl/fl}$ T cells were protected from EAE, recapitulating the protection seen in tamoxifen-treated, intact *UBC*$^{Cre/ERT2+}$*Ctla4*$^{fl/fl}$ mice (Fig. 3A). In this setting, we again observed expansion of both Treg and Tconv when *Ctla4* was deleted (data not shown). Thus, deletion of *Ctla4* on mature CD4$^+$ T cells can lead to EAE resistance.

The expansion of both Tconv and Treg populations upon CTLA-4 deletion led us to investigate the impact of *Ctla4* deletion on Tconv *versus* Treg. We first assessed

whether an antigen-specific Tconv population could transfer disease when *Ctla4* is deleted. To address this issue, we bred *UBC*$^{Cre/ERT2+}$*Ctla4*$^{fl/fl}$ mice to mice bearing the 2D2 transgenic T cell receptor (TCR), specific for MOG_{35-55}. We transferred 2D2 TCR transgenic $CD4^+$ T cells from *UBC*$^{Cre/ERT2-}$*Ctla4*$^{fl/fl}$ or *UBC*$^{Cre/ERT2+}$*Ctla4*$^{fl/fl}$ mice to *Rag1*$^{-/-}$ recipients and immunized with MOG_{35-55} concurrently with tamoxifen treatment. Both *2D2*$^+$*UBC*$^{Cre/ERT2+}$*Ctla4*$^{fl/fl}$ and *2D2*$^+$ *UBC*$^{Cre/ERT2-}$*Ctla4*$^{fl/fl}$ T cells were able to transfer disease (Fig. 3B). Additionally, we sorted $CD4^+$Foxp3-GFP^- T cells from non-TCR transgenic *UBC*$^{Cre/ERT2+}$*Ctla4*$^{fl/fl}$ and *UBC*$^{Cre/ERT2-}$*Ctla4*$^{fl/fl}$ mice and transferred these to $TCR\alpha^{-/-}$ recipients, which were then treated with tamoxifen and immunized with MOG_{35-55}. Both *UBC*$^{Cre/ERT2+}$*Ctla4*$^{fl/fl}$ and *UBC*$^{Cre/ERT2-}$*Ctla4*$^{fl/fl}$ $CD4^+$Foxp3-GFP^- T cells were able to induce disease (Fig. S5). Furthermore, *IL-17F*$^{Cre+}$*Ctla4*$^{fl/fl}$ mice, which were deleted for *Ctla4* on a subset of $CD4^+$ effector T cells, displayed identical disease susceptibility to their littermate controls (data not shown). Thus, effector $CD4^+$ T cells that lack *Ctla4* are able to become pathogenic and do not appear to be responsible for the EAE resistance of mice in which *Ctla4* is deleted during adulthood.

We next asked whether deletion of *Ctla4* only in the Treg compartment would recapitulate resistance to EAE. We bred the *Ctla4*$^{fl/fl}$ mouse to a *Foxp3*$^{eGFP/Cre/ERT2}$ mouse (Rubtsov et al., 2010) to enable tamoxifen-inducible deletion of *Ctla4* specifically on Treg. Tamoxifen treatment of adult mice resulted in deletion of CTLA-4 on $Foxp3^+$ Treg to a similar degree to that achieved in the *UBC*$^{Cre/ERT2+}$*Ctla4*$^{fl/fl}$ mice, while CTLA-4 expression on $CD4^+$Foxp3$^-$ cells was unchanged (Fig. 3C). After tamoxifen treatment, mice were immunized with MOG_{35-55} to induce EAE. EAE developed in control mice (either non-Cre-expressing *Ctla4*$^{fl/fl}$, *Foxp3*$^{eGFP/Cre/ERT2}$*Ctla4*$^{fl/+}$ or *Foxp3*$^{eGFP/Cre/ERT2}$*Ctla*$^{+/+}$

mice), but not in *Foxp3*$^{eGFP/Cre/ERT2}$*Ctla4*$^{fl/fl}$ mice (Fig. 3D and Table II). The degree of protection was profound and comparable to that observed in *UBC*$^{Cre/ERT2+}$*Ctla4*$^{fl/fl}$ mice. Thus, deletion of CTLA-4 specifically on Treg, during adulthood, leads to protection from induced autoimmunity.

CTLA-4 governs a Tconv-intrinsic effect on expansion

Since CTLA-4 deletion on Tconv alone failed to confer protection from EAE, we questioned whether there might be a functional role for CTLA-4 deletion on Tconv in a different setting. Taking advantage of the ability of our model to distinguish roles of CTLA-4 on Tconv versus Treg, we targeted deletion of CTLA-4 specifically to Tconv by transferring Treg from *UBC*$^{Cre/ERT2-}$ mice together with Tconv from either *UBC*$^{Cre/ERT2+}$*Ctla4*$^{fl/fl}$ or *UBC*$^{Cre/ERT2+}$*Ctla*$^{+/+}$ mice into TCRα$^{-/-}$ recipients that were subsequently treated with tamoxifen. Input Tconv were distinguished from Treg by the expression of a Cre reporter (ROSA26-tdTomato). We found that targeted deletion of CTLA-4 on Tconv led to expansion of Tconv, but not Treg (Fig. 4), suggesting that CTLA-4 expression on Tconv, while insufficient to confer disease protection, does restrain the homeostatic expansion of Tconv.

Treg deleted for CTLA-4 during adulthood are functional

Several studies have reported that CTLA-4 is necessary for Treg function. Therefore, we next assessed the function of Treg in which *Ctla4* was inducibly deleted using a combination of *in vitro* and *in vivo* assays. To assess the suppressive function of CTLA-4 deleted Tregs *in vitro*, we co-cultured wild-type versus CTLA-4 deleted Tregs (from

tamoxifen treated *UBC*$^{Cre/ERT2+}$*Ctla4*$^{fl/fl}$ mice) in the presence of wild-type Tconv and APCs (live dendritic cells), and stimulated with anti-CD3. In this assay, Tregs lacking CTLA-4 were able to suppress Tconv proliferation *in vitro*; suppression at a 1:1 ratio of Treg:Tconv was equal to controls, while a slight decrease in suppressive capacity of the deleted Tregs was observed at a 1:4 ratio (Fig. 5A).

To assess Treg function *in vivo*, we developed an assay for suppression of homeostatic proliferation in lymphopenic mice. Wild-type Tconv were transferred to *Rag1*$^{-/-}$ hosts in the presence or absence of co-transferred Treg from *UBC*$^{Cre/ERT2+}$*Ctla4*$^{fl/fl}$ or *UBC*$^{Cre/ERT2+}$*Ctla4*$^{+/+}$ mice. Recipient mice were treated with tamoxifen to induce CTLA-4 deletion in Tregs, and homeostatic proliferation of the transferred Tconv was quantitated 10 days following initial tamoxifen administration (on the day of transfer). We found that CTLA-4 deleted Treg were equivalent, if not better, than control Treg at suppressing homeostatic proliferation *in vivo* (Fig. 5B). The number of Treg obtained at the end of the assay was not significantly different between groups, suggesting that, on a per cell basis, CTLA-4-deficient Treg have suppressive capacity equal to that of control Treg. Taken together, these data indicate that Treg lacking CTLA-4 maintain their ability to suppress T cell proliferation *in vitro* and *in vivo*.

Treg lacking CTLA-4 impose an overabundance of IL-10 and increased expression of co-inhibitory receptors

Taken together, our data suggest that while deletion of CTLA-4 in mature T cells leads to increased activation of Tconv, these cells are rendered functionally impotent by the presence of Treg lacking CTLA-4, resulting in protection from EAE. To test this

hypothesis, we further characterized the phenotype of Tconv and Treg from UBC$^{Cre/ERT2+}$*Ctla4*$^{fl/fl}$ mice (in which CTLA-4 is deleted on both Tconv and Treg) by performing a focused transcriptional analysis of CTLA-4 deleted Tconv and Treg using a pathogenic Th17 Nanostring codeset (Lee et al., 2012; Yosef et al., 2013). *UBC*$^{Cre/ERT2+}$*Ctla4*$^{fl/fl}$ and *UBC*$^{Cre/ERT2-}$*Ctla4*$^{fl/fl}$ mice were treated with tamoxifen and immunized with MOG_{35-55}. At the peak of disease, RNA was isolated from Tconv and Treg sorted from spleen and cLN. We found that both Treg and Tconv populations adopt a gene expression signature associated with IL-10 production (Fig. S6). Among the most upregulated genes in *UBC*$^{Cre/ERT2+}$*Ctla4*$^{fl/fl}$ relative to *UBC*$^{Cre/ERT2-}$*Ctla4*$^{fl/fl}$ Tconv are *Ahr* (aryl-hydrocarbon receptor), *EBi3* (shared IL27/IL35 subunit) and *Icos*; each of these genes are involved in promoting the biology of IL-10 production and of type 1 regulatory-1 (Tr1) cells, an IL-10-producing, Foxp3-negative regulatory T cell population. When Treg are compared in a similar fashion, *Il10*, *Prdm1* (Blimp-1) and *Icos* are upregulated in *UBC*$^{Cre/ERT2+}$*Ctla4*$^{fl/fl}$ *versus UBC*$^{Cre/ERT2-}$*Ctla4*$^{fl/fl}$ samples, also suggesting that IL-10 production plays a significant functional role in conferring protection from EAE upon CTLA-4 deletion. Consistent with this hypothesis, we observe increased production of IL-10 by Tconv and Treg from CTLA-4-deleted mice, relative to Tconv from control mice, during EAE (Fig. 6A). Although *UBC*$^{Cre/ERT2+}$*Ctla4*$^{fl/fl}$ mice have a higher frequency of $CD4^+$ T cells from the cLN that produce the pathogenic cytokines IFN-γ and IL-17 compared to littermate controls (Fig. 6B), a larger proportion of each of these subsets additionally produces IL-10, relative to the corresponding cells from control mice (Fig. 6C). $CD4^+$ T cells lacking CTLA-4 also have increased surface expression of the co-inhibitory molecules Lag3 and PD-1 on both Tconv and Treg in the

cLN (Figs. 6D and 6E), as well as in the spleen (data not shown). Taken together, these data indicate that while CTLA-4 inhibits expansion of both Tconv and Treg, it also acts to inhibit IL-10 production and the expression of co-inhibitory receptors; hence, deletion of CTLA-4 results in overabundance of IL-10 and increased expression of co-inhibitory receptors, which mediates resistance to EAE.

Lastly, we asked whether loss of CTLA-4 on Treg alone was sufficient to induce the phenotypic changes in Tconv observed in *UBC*$^{Cre/ERT2+}$*Ctla4*$^{fl/fl}$ mice. Indeed, Treg from *Foxp3*$^{eGFP/Cre/ERT2}$*Ctla4*$^{fl/fl}$ mice treated with tamoxifen and immunized with MOG_{35-55} showed strikingly similar cellular phenotypes to those observed in *UBC*$^{Cre/ERT2+}$*Ctla4*$^{fl/fl}$ mice. At time points at which control mice had ongoing disease, the $CD4^+$ compartment of the cLN of *Foxp3*$^{eGFP/Cre/ERT2}$*Ctla4*$^{fl/fl}$ mice was as high as 60% $Foxp3^+$, indicating a massive accumulation of Treg (Fig. 7A). Moreover, both Treg and Tconv cells were increased in number in these mice (Fig. 7B), and both the CTLA-4-deleted Treg population and the CTLA-4 sufficient Tconv population displayed increased activation, as measured by the percentage of $CD62L^{lo}CD44^{hi}$ cells, and proliferation, as assessed by Ki-67 staining (Figs. 7C and 7D). Furthermore, expression of IL-10, Lag3 and PD-1 was increased in both T cell subsets (Figs. 7E-G). These findings confirm that the atypical pattern of Tconv activation, accompanied by increased expression of inhibitory molecules, that we observe in *UBC*$^{Cre/ERT2+}$*Ctla4*$^{fl/fl}$ mice, is driven by deletion of CTLA-4 specifically on Treg and independent of CTLA-4 expressed by Tconv.

Discussion

The dramatic, lethal phenotype of the germline CTLA-4 knockout mouse demonstrates the potency of this molecule as an inhibitory receptor (Tivol et al., 1995; Waterhouse et al., 1995). Since CTLA-4 is largely T cell-specific and constitutively expressed on Treg, but is also inducibly expressed on Tconv upon activation, the question of the relative contribution of CTLA-4 expression on Treg *versus* Tconv has been of great interest. In these studies, we have developed genetic approaches to address this question, uncoupling the role of CTLA-4 during development and in the adult immune system by utilizing inducible Cre systems that delete CTLA-4 either ubiquitously or specifically on $Foxp3^+$ Treg. By deleting CTLA-4 during adulthood, either on all cells or specifically on Treg, we have uncovered a surprising phenotype of resistance to spontaneous and induced autoimmune pathology. The underlying phenotype of T cells in these mice is one of apparent activation, coupled with Treg expansion but increased production of anti-inflammatory molecules. The distinct phenotype seen in our model, in contrast to that seen with non-inducible deletion of CTLA-4, may reflect necessary roles for CTLA-4 during the neonatal period, at which time Treg develop in and exit from the thymus (Asano et al., 1996). Since $Lck^{Cre+}Ctla4^{fl/fl}$ mice recapitulate the lethal phenotype of germline $Ctla4^{-/-}$ mice (data not shown), we hypothesize that inducible deletion of CTLA-4 during the neonatal period will recapitulate the germline knockout phenotype; however, such an analysis is beyond the scope of the present study.

Several groups have demonstrated that mice chimeric for wild-type and CTLA-4-deleted cells, either through adoptive transfer or bone marrow chimerism, are spared the lethal phenotype of germline CTLA-4 knockout mice (Bachmann et al., 1999;

Friedline et al., 2009). In our system, while CTLA-4 is deleted on the vast majority of cells, a small percentage of CTLA-4-expressing cells persists. We have treated *UBC*$^{Cre\text{-}ERT2+}$*Ctla4*$^{fl/fl}$ mice with a blocking monoclonal antibody against CTLA-4 following tamoxifen treatment, in an effort to neutralize the effect of any remaining CTLA-4^{+} cells, and have not observed any development of spontaneous autoimmunity or reversion of EAE protection in these experiments (data not shown). Furthermore, we observe similar frequencies of CTLA-4-deleted T cells in lymphoid organs and in the CNS during EAE progression (Fig. 2C), arguing against CTLA-4-sufficient cells having a competitive advantage in accessing or accumulating in the target organ.

We find that Treg with induced CTLA-4 deletion during adulthood are able to suppress Tconv proliferation both *in vitro* and *in vivo*. During the pathogenesis of EAE, we observe massive accumulation of Treg in the draining lymph node of CTLA-4-deleted mice, and an increased proportion of Treg in the CNS at early time points of disease. To explain the observed resistance to EAE in this setting, we propose that CTLA-4 on peripheral Treg acts as a brake to inhibit Treg proliferation. When CTLA-4 is absent, this constraint on Treg expansion is removed, and Treg accumulate dramatically, while remaining functionally competent. It has been shown that CD28 regulates peripheral homeostasis of Treg (Tang et al., 2003), and that Treg-specific deletion of CD28 leads to the generation of peripheral Treg that are unable to prevent autoimmunity (Zhang et al., 2013). Our findings likely reflect the converse situation; that is, loss of CTLA-4 leads to unrestrained CD28 signaling in Treg, resulting in Treg expansion and ultimately in EAE resistance.

CTLA-4-deficient Treg are capable of preventing pathogenic responses of Tconv, even if the Tconv themselves lack expression of CTLA-4. CTLA-4 deleted Treg may, in some respects, resemble tumor Treg, which are very potent suppressors and drive the development of dysfunctional/exhausted T cells. Interestingly, CTLA-4 deleted Treg have increased Lag3, PD-1 and IL-10 expression, similar to highly suppressive $TIM3^{+}$ Treg in the tumor microenvironment. As IL-10 has been implicated in development of T cell exhaustion during chronic viral infection, it is possible that IL-10 serves as one mechanism by which CTLA-4-deleted Treg could promote effector T cell dysfunction (Sakuishi et al., 2013). The type II IL-1 receptor IL-1R2, which indirectly reduces T cell activation through its function as a decoy receptor for IL-1a and IL-1b, is increased in CTLA-4 deleted Treg, suggesting another means by which CTLA-4 deleted Treg could impair Tconv function.

Importantly, the proposed role for CTLA-4 in inhibiting peripheral Treg expansion does not preclude it also functioning as a mediator of Treg suppression, as has been demonstrated by many groups. Our data suggest that CTLA-4 is not required for the ability of Treg to suppress Tconv proliferation, but that the net result of CTLA-4 loss *in vivo* leads to protection from EAE. It may be that increased proliferation of Treg, coupled with their increased production of anti-inflammatory cytokines, may compensate for a per-cell Treg dysfunction that would become apparent in other settings. CNS inflammation may be suppressible through CTLA-4-independent Treg mechanisms, such as IL-10 production, when Treg are present in sufficient numbers, which could explain why CTLA-4-deleted Treg are competent to suppress EAE. However, in other models, the *trans*-acting function of CTLA-4 to modulate B7-

expressing cells may be more important. Thus, there seem to be opposing roles for CTLA-4 on Treg: CTLA-4 appears to have an intrinsic function that acts as an inhibitor of Treg proliferation which, by virtue of the functional nature of Treg, counters its extrinsic function as a modulator of B7-expressing cells.

Our work does not reveal a necessary role for CTLA-4 on Tconv for the EAE resistance that we have observed; we do, however, observe a Tconv-intrinsic role for CTLA-4 in preventing T cell proliferation in our adoptive transfer experiments in which we target CTLA-4 deletion only to Foxp3^{-} populations. Since CTLA-4 deletion on T cells is likely to have an effect first on Treg (which constitutively express CTLA-4), the timing of tamoxifen administration relative to disease onset may be relevant. It may be that CTLA-4 deletion after activation of effector T cells would reveal a situation where the inhibitory effects of CTLA-4 on Tconv are more significant.

Our data point broadly toward the concept that co-inhibitory receptors expressed by Treg have inhibitory effects on the Treg themselves, with complex and, occasionally, paradoxical impact on the immune response in certain settings. The use of anti-CTLA-4 mAb to unleash an effective immune response against cancer is already an FDA-approved approach. However, the mechanisms by which these antibodies promote anti-tumor immunity are not yet fully understood, and some data suggest that the therapeutic effects of anti-CTLA-4 are being achieved through depletion of Treg (Bulliard et al., 2013; Simpson et al., 2013). Our data suggest that the use of a non-depleting anti-CTLA-4 antibody may, in fact, have undesired effects of promoting Treg proliferation and production of anti-inflammatory molecules. Such considerations will become increasingly important as the targeting of these molecules becomes a clinical reality.

Materials and Methods

Mice. Mice 6-10 weeks of age were used for all experiments. Wild-type C57BL/6 mice, *B6.Cg-Tg(UBC-cre/ERT2)1Ejb/J*, *B6.129S7-Rag1^{tm1Mom}/J*, *B6.SJL-Ptprc^{a} Pepc^{b}/BoyJ*, *B6.129S2-Tcra^{tm1Mom}/J* and *Foxp3$^{tm9(EGFP/cre/ERT2)Ayr}$*/J mice were purchased from The Jackson Laboratory. 2D2 TCR transgenic mice (Bettelli et al., 2003) and Foxp3-GFP reporter mice (Bettelli et al., 2006) were generated as described. All experimental mice were housed in specific pathogen-free conditions and used in accordance with animal care guidelines from the Harvard Medical School Standing Committee on Animals and the National Institutes of Health. Animal protocols were approved by the Harvard Medical School Standing Committee on Animals.

Antibodies and flow cytometry. Cells from lymphoid organs or CNS were isolated and resuspended in staining buffer (PBS containing 1% FCS and 2 mM EDTA) and were stained with the following directly labeled antibodies: anti-CD3 (145-2C11), anti-CD4 (RM4-5), anti-CD8α (53-6.7), anti-CD44 (IM7), anti-CD45.1 (A20), anti-CD45.2 (104), anti-CD62L (MEL-14), anti-IL-10 (JES5-16E3), anti-IL-17F (9D3.1C8), and anti-IFNγ (XMG1.2, all from BioLegend). 7-aminoactinomycin D (7-AAD; BioLegend) was used for exclusion of non-viable cells. For intracellular staining (anti-CTLA-4 (UC10-4B9, BD Biosciences); anti-Foxp3 (FJK-16, eBioscience); anti-Ki-67 (B56, BD BioSciences)), cells were fixed and permeabilized using the Foxp3/Transcription Factor Staining Kit (eBioscience) following surface staining, and LIVE/DEAD-Violet reagent (Life Technologies) was used for exclusion of non-viable cells. All flow cytometry data were

acquired on an LSR II cytometer with standard filter sets using FACSDiva software (BD Biosciences), and were further analyzed with FlowJo software (TreeStar).

Generation of conditional CTLA-4 knockout mouse. A conditional knockout targeting vector for the *Ctla4* gene was generated to contain three loxP sites: The first and second loxP sites flank a selection cassette consisting of a neomycin resistance gene (neo), under the control of the phosphoglycerate kinase (PGK) promoter and thymidine kinase (TK) under the control of the herpes simplex virus (HSV) promoter. This construct also contains diphtheria toxin (DTA) under the control of the PGK promoter, which allows for selection against non-homologous recombination events. Exons 2 and 3 of *Ctla4* were inserted into the vector downstream of the selection cassette and upstream of the third loxP site using a PCR-based approach, while the flanking regions of the *Ctla4* gene were cloned from a *Ctla4*-containing BAC using standard techniques. The targeting vector was introduced into C57BL/6 ES cells by electroporation and the resulting neomycin-resistant ES cells were screened for homologous recombination. ES cells carrying the desired homologous recombination event were subjected to a transient transfection with a Cre recombinase-expressing plasmid in order to remove the selection cassette. ES cells still containing the selection cassette were selected against using 1-(2-deoxy-2-fluoro-b-D-arabinofuranosyl)-5-iodouridine (FIAU) and ES cells retaining the two loxP sites flanking exons 2 and 3 were identified using a PCR-based approach and confirmed by genomic sequencing. Positive clones were micro-injected into albino-B6 blastocysts and implanted into pseudopregnant females to generate chimeras. Germ-line transmission of the ‘floxed’

Ctla4 allele was achieved and heterozygous mice were then bred to homozygosity. Breeding of *Ctla4*$^{fl/fl}$ mice to *B6.Cg-Tg(UBC-cre/ERT2)1Ejb/J* was performed to obtain tamoxifen-inducible deletion of *Ctla4* and to *Foxp3*$^{EGFP/Cre/ERT2}$ mice to obtain inducible deletion on Treg only.

Tamoxifen-induced conditional deletion in *UBC*$^{Cre/ERT2}$ mice. To prepare tamoxifen solution for injection, tamoxifen (Sigma) was dissolved in ethanol, diluted 1:20 in sunflower oil, and sonicated for 5 minutes at 37°C. Mice were injected daily with 1 mg tamoxifen intraperitoneally for 5 consecutive days, then rested for a minimum of 72 hours prior to any experimental manipulation.

EAE. MOG_{35-55} peptide (MEVGWYRSPFSRVVHLYRNGK) was synthesized at the Biopolymer Laboratory, Department of Neurology, David Geffen School of Medicine at UCLA; purity (>85%) was verified by HPLC. Amounts used were corrected for purity. To induce EAE, groups of 8-12 week old mice were immunized with 150 µg of MOG_{35-55} emulsified 1:1 in CFA with 400 µg of Mycobacterium tuberculosis H37RA (Difco Laboratories) in the two flanks subcutaneously. 250 ng of pertussis toxin (List Biological Laboratories) was injected intraperitoneally on the day of immunization and 2 d later. Mice were observed daily for clinical signs of EAE up to 30 d after immunization, and scored on a scale of 0–5: 0, no disease; 1, limp tail; 2, hind limb weakness; 3, hind limb paralysis; 4, hind and fore limb paralysis; and 5, moribund state. Mean clinical score was calculated by averaging the scores of all mice in each group, including animals that did not develop EAE.

Histopathology. Tissues were fixed in 10% formalin, and paraffin-embedded sections were stained with haematoxylin and eosin (H&E) or Luxol fast blue/periodic acid-Schiff (LFB-PAS) for light microscopic analysis. Photomicrographs were acquired on an Olympus BH-2 light microscope at the indicated magnifications using an Olympus DP71 camera and software provided by the manufacturer. Horizontal bars represent 200 µm for 100x images and 50 µm for 40x images. CNS pathology was scored blindly by a neuropathologist (R.A.S.). Inflammatory foci in meninges and parenchyma were counted as described previously (Sobel et al., 1990).

Gene expression quantitation by real-time quantitative PCR. Total RNA was isolated using the RNEasy Mini Plus Kit (QIAGEN) and quantitated using a NanoDrop 1000 spectrophotometer (Thermo Fisher). cDNA was synthesized by reverse transcription with random hexamer primers using the High Capacity cDNA Synthesis Kit (Applied Biosystems). Real-time qPCR was performed using SYBR Green chemistry (Roche) on a LightCycler 480 instrument; all samples were run in triplicate and no-template control (NTC) samples included for each gene to exclude DNA contamination. Primer sequences (CTLA-4 forward: 5'- AGAACCATGCCCGGATTCTG-3', CTLA-4 reverse: 5'- CATCTTGCTCAAAGAAACAGCAG-3') were obtained from PrimerBank (http://pga.mgh.harvard.edu/primerbank/) (Wang et al., 2012).

Gene expression quantitation by Nanostring analysis. Gene expression in sorted Tconv and Treg populations was quantified using a custom nCounter probe set

containing 301 probe pairs, including additional probes for positive and negative controls and housekeeping genes (NanoString Technologies)(Yosef et al., 2013). Briefly, total cellular RNA was isolated and quantitated as above, and 100 ng was hybridized with customized Reporter CodeSet and Capture ProbeSet (NanoString Technologies) by overnight incubation in a thermal cycler at 65°C. The next day, flow cell preparation and scanning were performed using an nCounter instrument (Nanostring Technologies) according to the manufacturer's instructions. Raw data were normalized using nSolver software (Nanostring Technologies) and exported as raw transcript counts for presentation. To normalize data, average background was subtracted from raw count, and normalization was performed using the geometric mean count from 4 housekeeping genes (*Gapdh*, *Hprt*, *Actb*, and *Tubb5*). Heat maps were generated using GENE-E software (http://www.broadinstitute.org/cancer/software/GENE-E/).

Analysis of CNS-infiltrating mononuclear cells. Prior to dissection, mice were perfused through the left ventricle with cold PBS. The brain and the spinal cord isolated, and CNS tissue was minced with a sharp razor blade and digested for 20 min at 37 °C with collagenase D (2.5 mg/ml; Roche) and DNaseI (1 mg/ml; Sigma). Mononuclear cells were isolated by passage of the tissue through a cell strainer (70 µm), followed by centrifugation through a Percoll gradient (37% and 70%). Mononuclear cells in the interphase were removed, washed and resuspended in culture medium for analysis.

Intracellular cytokine staining. Cells from lymphoid organs were isolated and restimulated with 50 ng/ml phorbol 12-myristate 13-acetate (PMA) and 500 ng/ml ionomycin (both from Sigma) in the presence of GolgiStop (BD Biosciences) for 4-5 hours, then processed for flow cytometric analysis as described above.

Adoptive transfers. Bulk $CD4^+$ (isolated from spleens by CD4 Microbeads; Miltenyi Biotec) or $CD4^+$Foxp3-GFP^- (isolated from spleens by fluorescence-activated cell sorting; FACS) were transferred to $TCR\alpha^{-/-}$ or $Rag1^{-/-}$ recipients that were then treated with tamoxifen and immunized with MOG_{35-55} to induce EAE.

In vitro **Treg suppression assay.** Responder Tconv were purified by sorting of $CD4^+CD62L^{hi}CD25^-$ T cells from $CD45.1^+$ congenic splenocytes and stained with CellTrace Violet Cell Proliferation Kit (Molecular Probes) according to the manufacturer's instructions. $CD4^+$Foxp3-GFP^+ Treg were purified by sorting from splenocytes from tamoxifen-treated *UBC*$^{Cre/ERT2+}$*Ctla4*$^{fl/fl}$ or *UBC*$^{Cre/ERT2-}$*Ctla4*$^{fl/fl}$ mice. Dendritic cells were isolated from wild-type C57BL/6 spleens that were collagenase-treated, using CD11c Microbeads and MACS columns (Miltenyi Biotec). Tconv and Treg were co-cultured at varying ratios, in the presence of 10% dendritic cells and 2 µg/ml anti-CD3, for three days. Co-cultures were then harvested and analyzed by flow-cytometry. Responder Tconv were gated on CD4 and CD45.1 ($7\text{-}AAD^+$ cells were excluded) and dilution of CellTrace Violet was assessed.

***In vivo* Treg suppression assay.** This assay was adapted from Workman et al (Workman et al., 2011). $CD4^+Foxp3\text{-}GFP^+$ cells were purified by sorting from lymphoid organs of *Foxp3-GFPKI* mice that were either $UBC^{Cre/ERT2+}Ctla4^{fl/fl}$ or $UBC^{Cre/ERT2+}Ctla4^{+/+}$. $CD4^+CD62L^{hi}CD25^-$ Tconv cells were purified by sorting from lymphoid organs of CD45.1 congenic mice. Treg and Tconv cells were adoptively co-transferred into $Rag1^{-/-}$ hosts, such that Treg cells comprised 25% of the total transferred cell population; a separate group of mice received T_{conv} cells alone (positive control). Recipients were treated with tamoxifen on days 0-4. Ten days after transfer, mice were sacrificed and $CD45.1^+CD4^+$ Tconv and $CD45.1^-CD4^+Foxp3\text{-}GFP^+$ Treg were quantitated by cell counting and flow cytometric analysis of splenocytes.

Statistical analysis. Prism software (GraphPad) was used for statistical analysis. Student's two- tailed *t*-test was used for all pairwise comparisons. Differences were considered statistically significant with a *p* value of 0.05 (*), 0.01 (**) or 0.001 (***).

Online supplemental material. Supplemental Figure 1 illustrates the strategy used to generate the CTLA-4 conditional knockout mouse. Supplemental Figure 2 demonstrates deletion of CTLA-4 in conditional knockout mice by qPCR. Supplemental Figure 3 demonstrates that CTLA-4 deletion during adulthood does not induce spontaneous disease. Supplemental Figure 4 illustrates histological EAE in CTLA-4 conditional knockout mice. Supplemental Figure 5 demonstrates that CTLA-4 deleted Tconv remain pathogenic, and are capable of inducing EAE following adoptive transfer to lymphopenic

hosts in the absence of Treg. Supplemental Figure 6 demonstrates transcriptional changes in CTLA-4 deleted Tconv and Treg.

Acknowledgments

The authors thank Justin Trombley for technical assistance; Baolin Chang, Xiaohui He, Vition Mbrica, Milagros Ávalo, and Louise Barias for assistance with mouse genotyping and colony maintenance; Vikram Juneja for experimental help and useful discussion; and Sarah Hillman for administrative support. This work was supported by grants from the National Institutes of Health (AI38310 and AI40614 to A.H.S.; P01 AI39671 to A.H.S. and V.K.K.; PO1 AI56299 to A.H.S., G.J.F, and V.K.K.) and the National Multiple Sclerosis Society (FG-1916-A-1 to S.B.L.). The authors declare no conflicts of interest.

References

Asano, M., M. Toda, N. Sakaguchi, and S. Sakaguchi. 1996. Autoimmune disease as a consequence of developmental abnormality of a T cell subpopulation. *J Exp Med*. 184:387-396.

Bachmann, M.F., G. Kohler, B. Ecabert, T.W. Mak, and M. Kopf. 1999. Cutting edge: lymphoproliferative disease in the absence of CTLA-4 is not T cell autonomous. *Journal of immunology*. 163:1128-1131.

Bettelli, E., Y. Carrier, W. Gao, T. Korn, T.B. Strom, M. Oukka, H.L. Weiner, and V.K. Kuchroo. 2006. Reciprocal developmental pathways for the generation of pathogenic effector TH17 and regulatory T cells. *Nature*. 441:235-238.

Bettelli, E., M. Pagany, H.L. Weiner, C. Linington, R.A. Sobel, and V.K. Kuchroo. 2003. Myelin oligodendrocyte glycoprotein-specific T cell receptor transgenic mice develop spontaneous autoimmune optic neuritis. *J Exp Med*. 197:1073-1081.

Buhlmann, J.E., S.K. Elkin, and A.H. Sharpe. 2003. A role for the B7-1/B7-2:CD28/CTLA-4 pathway during negative selection. *Journal of immunology*. 170:5421-5428.

Bulliard, Y., R. Jolicoeur, M. Windman, S.M. Rue, S. Ettenberg, D.A. Knee, N.S. Wilson, G. Dranoff, and J.L. Brogdon. 2013. Activating Fc gamma receptors contribute to the antitumor activities of immunoregulatory receptor-targeting antibodies. *J Exp Med*. 210:1685-1693.

Chambers, C.A., D. Cado, T. Truong, and J.P. Allison. 1997. Thymocyte development is normal in CTLA-4-deficient mice. *Proc Natl Acad Sci U S A*. 94:9296-9301.

Chuang, E., T.S. Fisher, R.W. Morgan, M.D. Robbins, J.M. Duerr, M.G. Vander Heiden, J.P. Gardner, J.E. Hambor, M.J. Neveu, and C.B. Thompson. 2000. The CD28 and CTLA-4 receptors associate with the serine/threonine phosphatase PP2A. *Immunity*. 13:313-322.

Chuang, E., K.M. Lee, M.D. Robbins, J.M. Duerr, M.L. Alegre, J.E. Hambor, M.J. Neveu, J.A. Bluestone, and C.B. Thompson. 1999. Regulation of cytotoxic T lymphocyte-associated molecule-4 by Src kinases. *Journal of immunology*. 162:1270-1277.

Cilio, C.M., M.R. Daws, A. Malashicheva, C.L. Sentman, and D. Holmberg. 1998. Cytotoxic T lymphocyte antigen 4 is induced in the thymus upon in vivo activation and its blockade prevents anti-CD3-mediated depletion of thymocytes. *J Exp Med*. 188:1239-1246.

Fallarino, F., U. Grohmann, K.W. Hwang, C. Orabona, C. Vacca, R. Bianchi, M.L. Belladonna, M.C. Fioretti, M.L. Alegre, and P. Puccetti. 2003. Modulation of tryptophan catabolism by regulatory T cells. *Nat Immunol*. 4:1206-1212.

Fife, B.T., and J.A. Bluestone. 2008. Control of peripheral T-cell tolerance and autoimmunity via the CTLA-4 and PD-1 pathways. *Immunological reviews*. 224:166-182.

Fraser, J.H., M. Rincon, K.D. McCoy, and G. Le Gros. 1999. CTLA4 ligation attenuates AP-1, NFAT and NF-kappaB activity in activated T cells. *European journal of immunology*. 29:838-844.

Freeman, G.J., F. Borriello, R.J. Hodes, H. Reiser, J.G. Gribben, J.W. Ng, J. Kim, J.M. Goldberg, K. Hathcock, G. Laszlo, and et al. 1993. Murine B7-2, an alternative CTLA4 counter-receptor that costimulates T cell proliferation and interleukin 2 production. *J Exp Med*. 178:2185-2192.

Freeman, G.J., G.S. Gray, C.D. Gimmi, D.B. Lombard, L.J. Zhou, M. White, J.D. Fingeroth, J.G. Gribben, and L.M. Nadler. 1991. Structure, expression, and T cell costimulatory activity of the murine homologue of the human B lymphocyte activation antigen B7. *J Exp Med*. 174:625-631.

Freeman, G.J., D.B. Lombard, C.D. Gimmi, S.A. Brod, K. Lee, J.C. Laning, D.A. Hafler, M.E. Dorf, G.S. Gray, H. Reiser, and et al. 1992. CTLA-4 and CD28 mRNA are coexpressed in most T cells after activation. Expression of CTLA-4 and CD28 mRNA does not correlate with the pattern of lymphokine production. *Journal of immunology*. 149:3795-3801.

Friedline, R.H., D.S. Brown, H. Nguyen, H. Kornfeld, J. Lee, Y. Zhang, M. Appleby, S.D. Der, J. Kang, and C.A. Chambers. 2009. CD4+ regulatory T cells require CTLA-4 for the maintenance of systemic tolerance. *J Exp Med*. 206:421-434.

Gough, S.C., L.S. Walker, and D.M. Sansom. 2005. CTLA4 gene polymorphism and autoimmunity. *Immunological reviews*. 204:102-115.

Greenwald, R.J., M.A. Oosterwegel, D. van der Woude, A. Kubal, D.A. Mandelbrot, V.A. Boussiotis, and A.H. Sharpe. 2002. CTLA-4 regulates cell cycle progression during a primary immune response. *European journal of immunology*. 32:366-373.

Harper, K., C. Balzano, E. Rouvier, M.G. Mattei, M.F. Luciani, and P. Golstein. 1991. CTLA-4 and CD28 activated lymphocyte molecules are closely related in both mouse and human as to sequence, message expression, gene structure, and chromosomal location. *Journal of immunology*. 147:1037-1044.

Hodi, F.S., S.J. O'Day, D.F. McDermott, R.W. Weber, J.A. Sosman, J.B. Haanen, R. Gonzalez, C. Robert, D. Schadendorf, J.C. Hassel, W. Akerley, A.J. van den Eertwegh, J. Lutzky, P. Lorigan, J.M. Vaubel, G.P. Linette, D. Hogg, C.H. Ottensmeier, C. Lebbe, C. Peschel, I. Quirt, J.I. Clark, J.D. Wolchok, J.S. Weber, J. Tian, M.J. Yellin, G.M. Nichol, A. Hoos, and W.J. Urba. 2010. Improved survival with ipilimumab in patients with metastatic melanoma. *The New England journal of medicine*. 363:711-723.

Ise, W., M. Kohyama, K.M. Nutsch, H.M. Lee, A. Suri, E.R. Unanue, T.L. Murphy, and K.M. Murphy. 2010. CTLA-4 suppresses the pathogenicity of self antigen-specific T cells by cell-intrinsic and cell-extrinsic mechanisms. *Nat Immunol*. 11:129-135.

Jain, N., H. Nguyen, C. Chambers, and J. Kang. 2010. Dual function of CTLA-4 in regulatory T cells and conventional T cells to prevent multiorgan autoimmunity. *Proc Natl Acad Sci U S A*. 107:1524-1528.

Kong, K.F., G. Fu, Y. Zhang, T. Yokosuka, J. Casas, A.J. Canonigo-Balancio, S. Becart, G. Kim, J.R. Yates, 3rd, M. Kronenberg, T. Saito, N.R. Gascoigne, and A. Altman. 2014. Protein kinase C-eta controls CTLA-4-mediated regulatory T cell function. *Nat Immunol*. 15:465-472.

Krummel, M.F., and J.P. Allison. 1996. CTLA-4 engagement inhibits IL-2 accumulation and cell cycle progression upon activation of resting T cells. *J Exp Med*. 183:2533-2540.

Lee, K.M., E. Chuang, M. Griffin, R. Khattri, D.K. Hong, W. Zhang, D. Straus, L.E. Samelson, C.B. Thompson, and J.A. Bluestone. 1998. Molecular basis of T cell inactivation by CTLA-4. *Science*. 282:2263-2266.

Lee, Y., A. Awasthi, N. Yosef, F.J. Quintana, S. Xiao, A. Peters, C. Wu, M. Kleinewietfeld, S. Kunder, D.A. Hafler, R.A. Sobel, A. Regev, and V.K. Kuchroo. 2012. Induction and molecular signature of pathogenic TH17 cells. *Nat Immunol*. 13:991-999.

Linsley, P.S., W. Brady, M. Urnes, L.S. Grosmaire, N.K. Damle, and J.A. Ledbetter. 1991. CTLA-4 is a second receptor for the B cell activation antigen B7. *J Exp Med*. 174:561-569.

Linsley, P.S., J.L. Greene, P. Tan, J. Bradshaw, J.A. Ledbetter, C. Anasetti, and N.K. Damle. 1992. Coexpression and functional cooperation of CTLA-4 and CD28 on activated T lymphocytes. *J Exp Med*. 176:1595-1604.

Liu, Z., K. Geboes, P. Hellings, P. Maerten, H. Heremans, P. Vandenberghe, L. Boon, P. van Kooten, P. Rutgeerts, and J.L. Ceuppens. 2001. B7 interactions with CD28 and CTLA-4 control tolerance or induction of mucosal inflammation in chronic experimental colitis. *Journal of immunology*. 167:1830-1838.

Marengere, L.E., P. Waterhouse, G.S. Duncan, H.W. Mittrucker, G.S. Feng, and T.W. Mak. 1996. Regulation of T cell receptor signaling by tyrosine phosphatase SYP association with CTLA-4. *Science*. 272:1170-1173.

Metzler, B., C. Burkhart, and D.C. Wraith. 1999. Phenotypic analysis of CTLA-4 and CD28 expression during transient peptide-induced T cell activation in vivo. *International immunology*. 11:667-675.

Olsson, C., K. Riesbeck, M. Dohlsten, and E. Michaelsson. 1999. CTLA-4 ligation suppresses CD28-induced NF-kappaB and AP-1 activity in mouse T cell blasts. *J Biol Chem*. 274:14400-14405.

Onishi, Y., Z. Fehervari, T. Yamaguchi, and S. Sakaguchi. 2008. Foxp3+ natural regulatory T cells preferentially form aggregates on dendritic cells in vitro and actively inhibit their maturation. *Proc Natl Acad Sci U S A*. 105:10113-10118.

Punt, J.A., W. Havran, R. Abe, A. Sarin, and A. Singer. 1997. T cell receptor (TCR)-induced death of immature CD4+CD8+ thymocytes by two distinct mechanisms differing in their requirement for CD28 costimulation: implications for negative selection in the thymus. *J Exp Med*. 186:1911-1922.

Punt, J.A., B.A. Osborne, Y. Takahama, S.O. Sharrow, and A. Singer. 1994. Negative selection of CD4+CD8+ thymocytes by T cell receptor-induced apoptosis requires a costimulatory signal that can be provided by CD28. *J Exp Med*. 179:709-713.

Qureshi, O.S., Y. Zheng, K. Nakamura, K. Attridge, C. Manzotti, E.M. Schmidt, J. Baker, L.E. Jeffery, S. Kaur, Z. Briggs, T.Z. Hou, C.E. Futter, G. Anderson, L.S. Walker, and D.M. Sansom. Trans-endocytosis of CD80 and CD86: a molecular basis for the cell-extrinsic function of CTLA-4. *Science*. 332:600-603.

Read, S., R. Greenwald, A. Izcue, N. Robinson, D. Mandelbrot, L. Francisco, A.H. Sharpe, and F. Powrie. 2006. Blockade of CTLA-4 on CD4+CD25+ regulatory T cells abrogates their function in vivo. *Journal of immunology*. 177:4376-4383.

Read, S., V. Malmstrom, and F. Powrie. 2000. Cytotoxic T lymphocyte-associated antigen 4 plays an essential role in the function of CD25(+)CD4(+) regulatory cells that control intestinal inflammation. *J Exp Med*. 192:295-302.

Robert, C., L. Thomas, I. Bondarenko, S. O'Day, D.J. M, C. Garbe, C. Lebbe, J.F. Baurain, A. Testori, J.J. Grob, N. Davidson, J. Richards, M. Maio, A. Hauschild, W.H. Miller, Jr., P. Gascon, M. Lotem, K. Harmankaya, R. Ibrahim, S. Francis, T.T. Chen, R. Humphrey, A. Hoos, and J.D. Wolchok. 2011. Ipilimumab plus dacarbazine for previously untreated metastatic melanoma. *The New England journal of medicine*. 364:2517-2526.

Rubtsov, Y.P., R.E. Niec, S. Josefowicz, L. Li, J. Darce, D. Mathis, C. Benoist, and A.Y. Rudensky. 2010. Stability of the regulatory T cell lineage in vivo. *Science*. 329:1667-1671.

Sakuishi, K., S.F. Ngiow, J.M. Sullivan, M.W. Teng, V.K. Kuchroo, M.J. Smyth, and A.C. Anderson. 2013. TIM3FOXP3 regulatory T cells are tissue-specific promoters of T-cell dysfunction in cancer. *Oncoimmunology*. 2:e23849.

Salomon, B., D.J. Lenschow, L. Rhee, N. Ashourian, B. Singh, A. Sharpe, and J.A. Bluestone. 2000. B7/CD28 costimulation is essential for the homeostasis of the

CD4+CD25+ immunoregulatory T cells that control autoimmune diabetes. *Immunity*. 12:431-440.

Scalapino, K.J., and D.I. Daikh. 2008. CTLA-4: a key regulatory point in the control of autoimmune disease. *Immunological reviews*. 223:143-155.

Schmidt, E.M., C.J. Wang, G.A. Ryan, L.E. Clough, O.S. Qureshi, M. Goodall, A.K. Abbas, A.H. Sharpe, D.M. Sansom, and L.S. Walker. 2009. Ctla-4 controls regulatory T cell peripheral homeostasis and is required for suppression of pancreatic islet autoimmunity. *Journal of immunology*. 182:274-282.

Sharpe, A.H., and G.J. Freeman. 2002. The B7-CD28 superfamily. *Nat Rev Immunol*. 2:116-126.

Simpson, T.R., F. Li, W. Montalvo-Ortiz, M.A. Sepulveda, K. Bergerhoff, F. Arce, C. Roddie, J.Y. Henry, H. Yagita, J.D. Wolchok, K.S. Peggs, J.V. Ravetch, J.P. Allison, and S.A. Quezada. 2013. Fc-dependent depletion of tumor-infiltrating regulatory T cells co-defines the efficacy of anti-CTLA-4 therapy against melanoma. *J Exp Med*. 210:1695-1710.

Sobel, R.A., V.K. Tuohy, Z.J. Lu, R.A. Laursen, and M.B. Lees. 1990. Acute experimental allergic encephalomyelitis in SJL/J mice induced by a synthetic peptide of myelin proteolipid protein. *Journal of neuropathology and experimental neurology*. 49:468-479.

Tai, X., M. Cowan, L. Feigenbaum, and A. Singer. 2005. CD28 costimulation of developing thymocytes induces Foxp3 expression and regulatory T cell differentiation independently of interleukin 2. *Nat Immunol*. 6:152-162.

Tai, X., F. Van Laethem, L. Pobezinsky, T. Guinter, S.O. Sharrow, A. Adams, L. Granger, M. Kruhlak, T. Lindsten, C.B. Thompson, L. Feigenbaum, and A. Singer. 2012. Basis of CTLA-4 function in regulatory and conventional CD4(+) T cells. *Blood*. 119:5155-5163.

Takahashi, S., H. Kataoka, S. Hara, T. Yokosuka, K. Takase, S. Yamasaki, W. Kobayashi, Y. Saito, and T. Saito. 2005. In vivo overexpression of CTLA-4 suppresses lymphoproliferative diseases and thymic negative selection. *European journal of immunology*. 35:399-407.

Takahashi, T., T. Tagami, S. Yamazaki, T. Uede, J. Shimizu, N. Sakaguchi, T.W. Mak, and S. Sakaguchi. 2000. Immunologic self-tolerance maintained by CD25(+)CD4(+) regulatory T cells constitutively expressing cytotoxic T lymphocyte-associated antigen 4. *J Exp Med*. 192:303-310.

Tang, Q., E.K. Boden, K.J. Henriksen, H. Bour-Jordan, M. Bi, and J.A. Bluestone. 2004. Distinct roles of CTLA-4 and TGF-beta in CD4+CD25+ regulatory T cell function. *European journal of immunology*. 34:2996-3005.

Tang, Q., K.J. Henriksen, E.K. Boden, A.J. Tooley, J. Ye, S.K. Subudhi, X.X. Zheng, T.B. Strom, and J.A. Bluestone. 2003. Cutting edge: CD28 controls peripheral homeostasis of CD4+CD25+ regulatory T cells. *Journal of immunology*. 171:3348-3352.

Tivol, E.A., F. Borriello, A.N. Schweitzer, W.P. Lynch, J.A. Bluestone, and A.H. Sharpe. 1995. Loss of CTLA-4 leads to massive lymphoproliferation and fatal multiorgan tissue destruction, revealing a critical negative regulatory role of CTLA-4. *Immunity*. 3:541-547.

Ueda, H., J.M. Howson, L. Esposito, J. Heward, H. Snook, G. Chamberlain, D.B. Rainbow, K.M. Hunter, A.N. Smith, G. Di Genova, M.H. Herr, I. Dahlman, F. Payne, D. Smyth, C. Lowe, R.C. Twells, S. Howlett, B. Healy, S. Nutland, H.E. Rance, V. Everett, L.J. Smink, A.C. Lam, H.J. Cordell, N.M. Walker, C. Bordin, J. Hulme, C. Motzo, F. Cucca, J.F. Hess, M.L. Metzker, J. Rogers, S. Gregory, A. Allahabadia, R. Nithiyananthan, E. Tuomilehto-Wolf, J. Tuomilehto, P. Bingley, K.M. Gillespie, D.E. Undlien, K.S. Ronningen, C. Guja, C. Ionescu-Tirgoviste, D.A. Savage, A.P. Maxwell, D.J. Carson, C.C. Patterson, J.A. Franklyn, D.G. Clayton, L.B. Peterson, L.S. Wicker, J.A. Todd, and S.C. Gough. 2003. Association of the T-cell regulatory gene CTLA4 with susceptibility to autoimmune disease. *Nature*. 423:506-511.

Verhagen, J., L. Gabrysova, S. Minaee, C.A. Sabatos, G. Anderson, A.H. Sharpe, and D.C. Wraith. 2009. Enhanced selection of FoxP3+ T-regulatory cells protects CTLA-4-deficient mice from CNS autoimmune disease. *Proc Natl Acad Sci U S A*. 106:3306-3311.

Verhagen, J., R. Genolet, G.J. Britton, B.J. Stevenson, C.A. Sabatos-Peyton, J. Dyson, I.F. Luescher, and D.C. Wraith. 2013. CTLA-4 controls the thymic development of both conventional and regulatory T cells through modulation of the TCR repertoire. *Proc Natl Acad Sci U S A*. 110:E221-230.

Wagner, D.H., Jr., J. Hagman, P.S. Linsley, W. Hodsdon, J.H. Freed, and M.K. Newell. 1996. Rescue of thymocytes from glucocorticoid-induced cell death mediated by CD28/CTLA-4 costimulatory interactions with B7-1/B7-2. *J Exp Med*. 184:1631-1638.

Walker, L.S. 2013. Treg and CTLA-4: two intertwining pathways to immune tolerance. *Journal of autoimmunity*. 45:49-57.

Walunas, T.L., C.Y. Bakker, and J.A. Bluestone. 1996. CTLA-4 ligation blocks CD28-dependent T cell activation. *J Exp Med*. 183:2541-2550.

Wang, X., A. Spandidos, H. Wang, and B. Seed. 2012. PrimerBank: a PCR primer database for quantitative gene expression analysis, 2012 update. *Nucleic acids research*. 40:D1144-1149.

Waterhouse, P., J.M. Penninger, E. Timms, A. Wakeham, A. Shahinian, K.P. Lee, C.B. Thompson, H. Griesser, and T.W. Mak. 1995. Lymphoproliferative disorders with early lethality in mice deficient in Ctla-4. *Science*. 270:985-988.

Wing, K., Y. Onishi, P. Prieto-Martin, T. Yamaguchi, M. Miyara, Z. Fehervari, T. Nomura, and S. Sakaguchi. 2008. CTLA-4 control over Foxp3+ regulatory T cell function. *Science*. 322:271-275.

Workman, C.J., L.W. Collison, M. Bettini, M.R. Pillai, J.E. Rehg, and D.A. Vignali. 2011. In vivo Treg suppression assays. *Methods in molecular biology*. 707:119-156.

Wu, Y., M. Borde, V. Heissmeyer, M. Feuerer, A.D. Lapan, J.C. Stroud, D.L. Bates, L. Guo, A. Han, S.F. Ziegler, D. Mathis, C. Benoist, L. Chen, and A. Rao. 2006. FOXP3 controls regulatory T cell function through cooperation with NFAT. *Cell*. 126:375-387.

Yosef, N., A.K. Shalek, J.T. Gaublomme, H. Jin, Y. Lee, A. Awasthi, C. Wu, K. Karwacz, S. Xiao, M. Jorgolli, D. Gennert, R. Satija, A. Shakya, D.Y. Lu, J.J. Trombetta, M.R. Pillai, P.J. Ratcliffe, M.L. Coleman, M. Bix, D. Tantin, H. Park, V.K. Kuchroo, and A. Regev. 2013. Dynamic regulatory network controlling TH17 cell differentiation. *Nature*. 496:461-468.

Zhang, R., A. Huynh, G. Whitcher, J. Chang, J.S. Maltzman, and L.A. Turka. 2013. An obligate cell-intrinsic function for CD28 in Tregs. *The Journal of clinical investigation*. 123:580-593.

Zheng, Y., S.Z. Josefowicz, A. Kas, T.T. Chu, M.A. Gavin, and A.Y. Rudensky. 2007. Genome-wide analysis of Foxp3 target genes in developing and mature regulatory T cells. *Nature*. 445:936-940.

Figure Legends

Figure 1. Deletion of CTLA-4 induces resistance to EAE. *Ctla4*$^{fl/fl}$ mice that were either *UBC*$^{Cre/ERT2-}$ (Cre^{-}) or *UBC*$^{Cre/ERT2+}$ (Cre^{+}) were treated with tamoxifen and assessed for CTLA-4 expression by intracellular staining before immunization (A) or immunized with MOG_{35-55} to induce EAE (B). Data are representative of at least three independent experiments (mean and s.e.m. for at least 7 mice per group).

Figure 2. Deletion of CTLA-4 leads to expanded and apparently activated T cell populations. CD4^{+} cells from mice immunized with MOG_{35-55} to induce EAE were analyzed at the peak (A-D) or onset (E) of disease for (A) the number of Foxp3^{-} and Foxp3^{+} cells, (B) the percentage of Foxp3^{+} cells, (C) intracellular staining for Ki-67, and (D) surface staining for CD62L and CD44 within the cervical lymph node. (E) Brains and spinal cords from MOG_{35-55} immunized mice were analyzed at the onset of disease. Data are gated on CD4^{+} T cells. Data are representative of at least two independent experiments (mean and s.e.m. for at least 7 mice per group).

Figure 3. Dependence on deletion of CTLA-4 on Treg for resistance to EAE. (A) CD4^{+} cells or (B) 2D2^{+}CD4^{+} cells from *UBC*$^{Cre/ERT2-}$ (Cre^{-}) or *UBC*$^{Cre/ERT2+}$ (Cre^{+}) donors were adoptively transferred to (A) TCRα$^{-/-}$ or (B) Rag1$^{-/-}$ hosts, which were treated with tamoxifen and immunized with MOG_{35-55} to induce EAE. (C+D) Mice that were either *Foxp3*$^{eGFP/Cre/ERT2-}$ (Cre^{-}) or *Foxp3*$^{eGFP/Cre/ERT2+}$ (Cre^{+}) and that had either one (*Ctla4*$^{fl/+}$) or two (*Ctla4*$^{fl/fl}$) conditional knockout *Ctla4* alleles were treated with tamoxifen and

immunized with MOG_{35-55} to induce EAE. Cervical lymph node $CD4^+$ T cells were analyzed by intracellular staining for CTLA-4 protein (C) and mice were monitored for clinical disease (D). Data are representative of at least two independent experiments (n ≥ 5 mice per group).

Figure 4. Specific deletion of CTLA-4 on Tconv leads to increased Tconv-specific homeostatic expansion. *$CD4^+Foxp3\text{-}GFP^+$* cells from *$UBC^{Cre/ERT2-}Ctla4^{fl/fl}$* mice were transferred with *$CD4^+Foxp3\text{-}GFP^-$* cells from either *$UBC^{Cre/ERT2+}Ctla4^+ROSA26^{loxP\text{-}STOP\text{-}loxP\text{-}tdTomato}$* ('WT) or *$UBC^{Cre/ERT2+}Ctla4^{fl/fl}ROSA26^{loxP\text{-}STOP\text{-}loxP\text{-}tdTomato}$* ('DEL') mice to *$TCR\alpha^{-/-}$* recipients, which were subsequently treated with tamoxifen and immunized with MOG_{35-55}. Treg and Tconv were quantified in the spleen. Data are representative of three independent experiments (n ≥ 4 mice per group).

Figure 5. Treg lacking CTLA-4 are functional *in vitro* and *in vivo*. (A) Wildtype sorted $CD4^+CD62L^{hi}CD25^-$ T cells from $CD45.1^+$ congenic splenocytes (Tconv) were labelled with CellTrace Violet and co-cultured with sorted $CD4^+Foxp3\text{-}GFP^+$ Treg from *$UBC^{Cre/ERT2+}Ctla4^{fl/fl}$* (Cre+) or *$UBC^{Cre/ERT2-}Ctla4^{fl/fl}$* (Cre-) mice at the indicated ratios. Cells were cultured in the presence of wild-type dendritic cells and soluble anti-CD3 for 3 days. Percent suppression was calculated relative to samples with no Treg based on dilution of CellTrace Violet dilution. Right panel shows representative CellTrace histograms for a 1:1 ratio of Treg:Tconv and no Treg control (data are pooled from two independent experiments; five sorted Treg populations per group (each from 2-3 pooled mice)). (B) CD45.1 Tconv ($CD4^+CD62L^{hi}CD25^-$) were transferred to $Rag1^{-/-}$ recipients

with or without co-transfer of Treg from *UBC*$^{Cre/ERT2+}$*Ctla4*$^{fl/fl}$ or *UBC*$^{Cre/ERT2+}$*Ctla4*$^{+/+}$ mice and then treated with tamoxifen. Spleens were harvested on day 10 post-transfer and the number of Tconv (left panel) and Treg (right panel) were quantitated (n = 4 mice per group).

Figure 6. Deletion of CTLA-4 during adulthood leads to increased IL-10, PD-1 and Lag3 expression. CD4^{+} cells from *UBC*$^{Cre/ERT2+}$*Ctla4*$^{fl/fl}$ or *UBC*$^{Cre/ERT2-}$*Ctla4*$^{fl/fl}$ mice were immunized with MOG_{35-55} to induce EAE and analyzed at the peak of disease for cytokine production by intracellular staining. (A) Quantitation of IL-10 expression by Tconv (Foxp3^{-}) and Treg (Foxp3^{+}) splenocytes. (B) Quantitation of lFNγ and IL-17F production by Tconv (C) and IL-10 production among lFNγ- and IL-17F-producing Tconv (i.e., “double positive”) (D) in cLN. Data are gated on CD4^{+} T cells and are representative of at least two independent experiments (mean and s.e.m. for 4-6 mice per group).

Figure 7. Treg lacking CTLA-4 impose a phenotype of increased IL-10, PD-1 and Lag3 expression on Tconv. Mice that were *Foxp3*$^{eGFP/Cre/ERT2+}$ and that had either one (*Ctla4*$^{fl/+}$) or two (*Ctla4*$^{fl/fl}$) conditional knockout *Ctla4* alleles were treated with tamoxifen and immunized with MOG_{35-55} to induce EAE. Mice were analyzed at peak of disease for (A) the percentage of Foxp3^{+} cells, (B) the number of Foxp3^{-} and Foxp3^{+} cells, (C) surface staining for CD62L and CD44, (D) intracellular staining for Ki-67, (E) intracellular staining for IL-10, (F) surface staining for PD-1, (G) surface staining for Lag-3. Data are representative of three independent experiments.

Tables

Table I. *EAE in UBC-Cre^{ERT2} mice with induced deletion of CTLA-4*

	Clinical EAE*			Histological EAE			
	Incidence	Day of onset	Mean maximal score	Incidence	Meningeal foci	Parenchymal foci	Total foci
		Mean ± SE	*Mean ± SE*		*Mean ± SE*	*Mean ± SE*	*Mean ± SE*
Cre- (all)	41/49 (83.7%)	13.9 ± 0.4	2.2 ± 0.4	11/11 (100%)	55.5 ± 13.9	69.5 ± 23.5	125.2 ± 36.9
Cre+ (sunflower oil)	5/5 (100%)	13.0 ± 0.7	3.5 ± 0.2	4/4 (100%)	106 ± 11.8	99.8 ± 12.8	205.8 ± 23.2
Cre+ (tamoxifen)	16/44 (36.4%)	14.1 ± 1.0	0.4 ± 0.3 ($p < 0.0001$)†	12/13 (92.3%)	10.2 ± 3.8 ($p = 0.003$)	5.5 ± 2.3 ($p = 0.007$)	15.6 ± 5.7 ($p = 0.004$)

*Data are pooled from four independent experiments in which EAE was induced by immunization with 150 µg MOG 35-55 subcutaneously, and administration of 250 ng pertussis toxin intraperitoneally on the day of immunization and two days later. Mice with no disease were included in calculations of maximal score and histological EAE, but excluded from calculations of day of disease onset.
†All p values are compared with Cre- control.

Table II. *EAE in Foxp3-Cre^{ERT2} mice with Treg-specific induced deletion of CTLA-4*

	Clinical EAE*		
	Incidence	Day of onset	Mean maximal score
		Mean ± SE	*Mean ± SE*
Cre- CTLA-4$^{fl/fl}$	7/8 (87.5%)	11.9 ± 0.5	2.9 ± 0.5
Cre+ CTLA-4$^{+/+}$	2/2 (100%)	10.5 ± 0.5	3.3 ± 0.8
Cre+ CTLA-4$^{fl/+}$	12/13 (92.3%)	12.0 ± 1.1	2.7 ± 0.3
Cre+ CTLA-4$^{fl/fl}$	2/16 (12.5%)	14.0 ± 4.0	0.3 ± 0.2 ($p < 0.0001$)†

*Data are pooled from three independent experiments in which EAE was induced by immunization with 150 μg MOG 35-55 subcutaneously, and administration of 250 ng pertussis toxin intraperitoneally on the day of immunization and two days later. Mice with no disease were included in calculations of maximal score, but excluded from calculations of day of disease onset.
†All p values are compared with Cre- control.

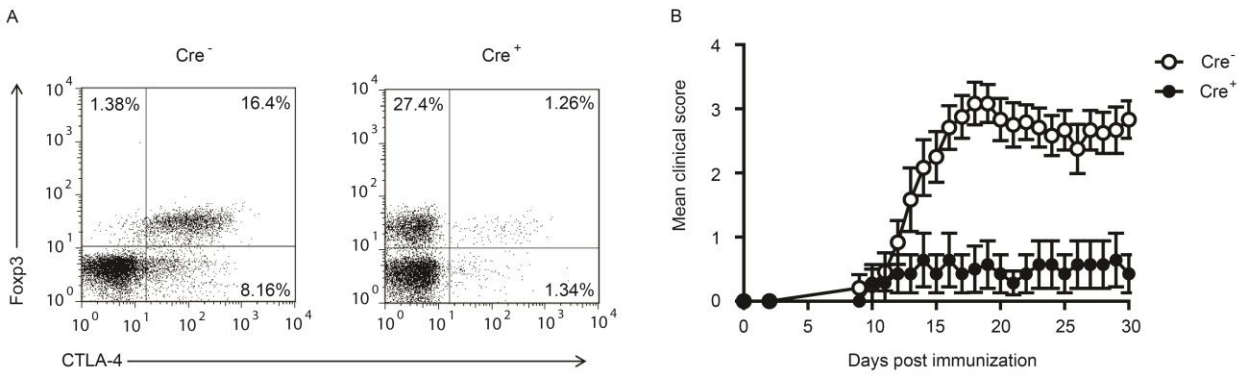
A
Cre-
Cre+
1.38%
16.4%
8.16%
27.4%
1.26%
1.34%
Foxp3
CTLA-4
B
Mean clinical score
Days post immunization
Cre-
Cre+

Figure 1

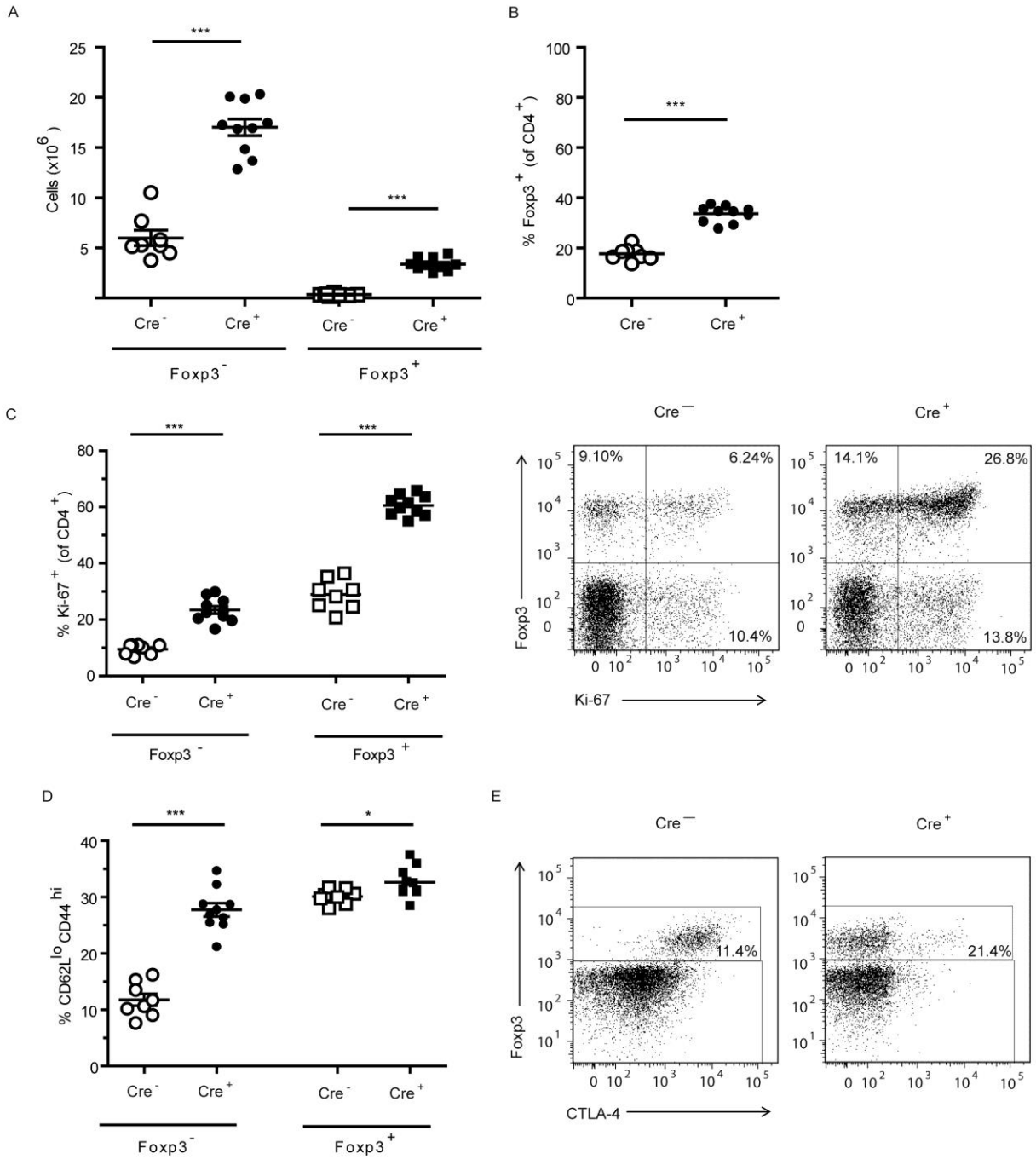
A
B
C
D
E
Cells (x10^6)
% Foxp3+ (of CD4+)
% Ki-67+ (of CD4+)
% CD62L^lo CD44^hi
Cre-
Cre+
Foxp3-
Foxp3+
Foxp3
Ki-67
CTLA-4
9.10%
6.24%
10.4%
14.1%
26.8%
13.8%
11.4%
21.4%

Figure 2

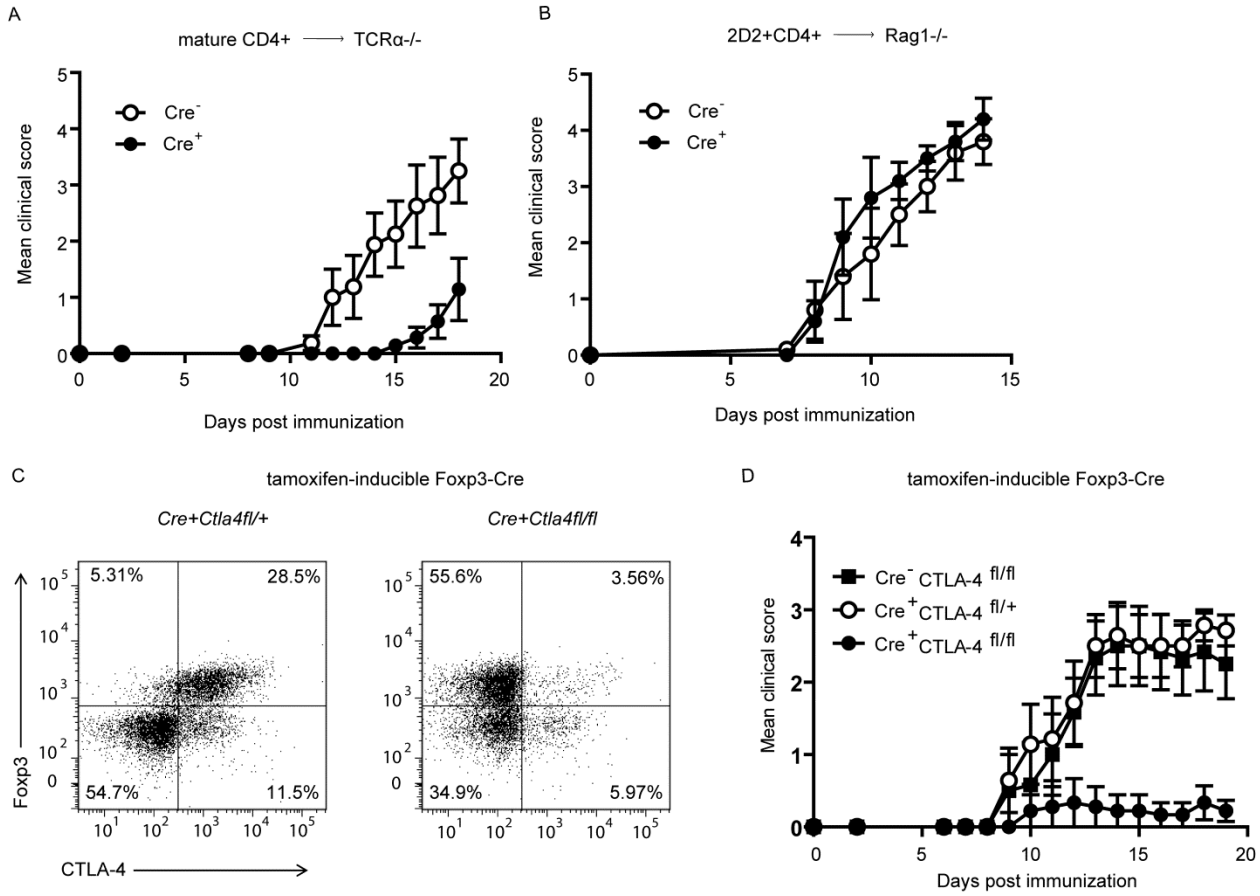
A
mature CD4+ ⟶ TCRα-/-
Mean clinical score
Cre⁻
Cre⁺
Days post immunization
B
2D2+CD4+ ⟶ Rag1-/-
Mean clinical score
Cre⁻
Cre⁺
Days post immunization
C
tamoxifen-inducible Foxp3-Cre
Cre+Ctla4fl/+
Cre+Ctla4fl/fl
5.31%
28.5%
54.7%
11.5%
55.6%
3.56%
34.9%
5.97%
Foxp3
CTLA-4
D
tamoxifen-inducible Foxp3-Cre
Mean clinical score
Cre⁻ CTLA-4 fl/fl
Cre⁺ CTLA-4 fl/+
Cre⁺ CTLA-4 fl/fl
Days post immunization

Figure 3

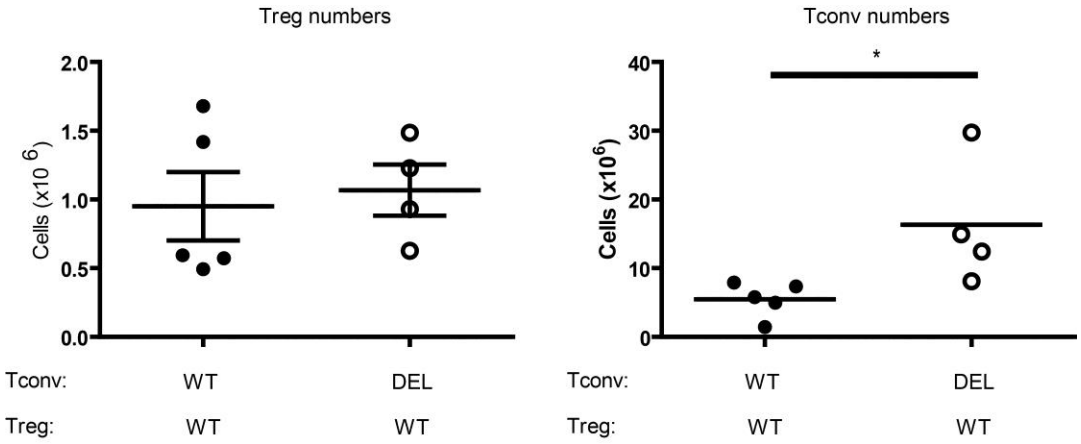
Treg numbers
Cells (x10 6)
2.0
1.5
1.0
0.5
0.0
Tconv: WT DEL
Treg: WT WT
Tconv numbers
*
Cells (x10^6)
40
30
20
10
0
Tconv: WT DEL
Treg: WT WT

Figure 4

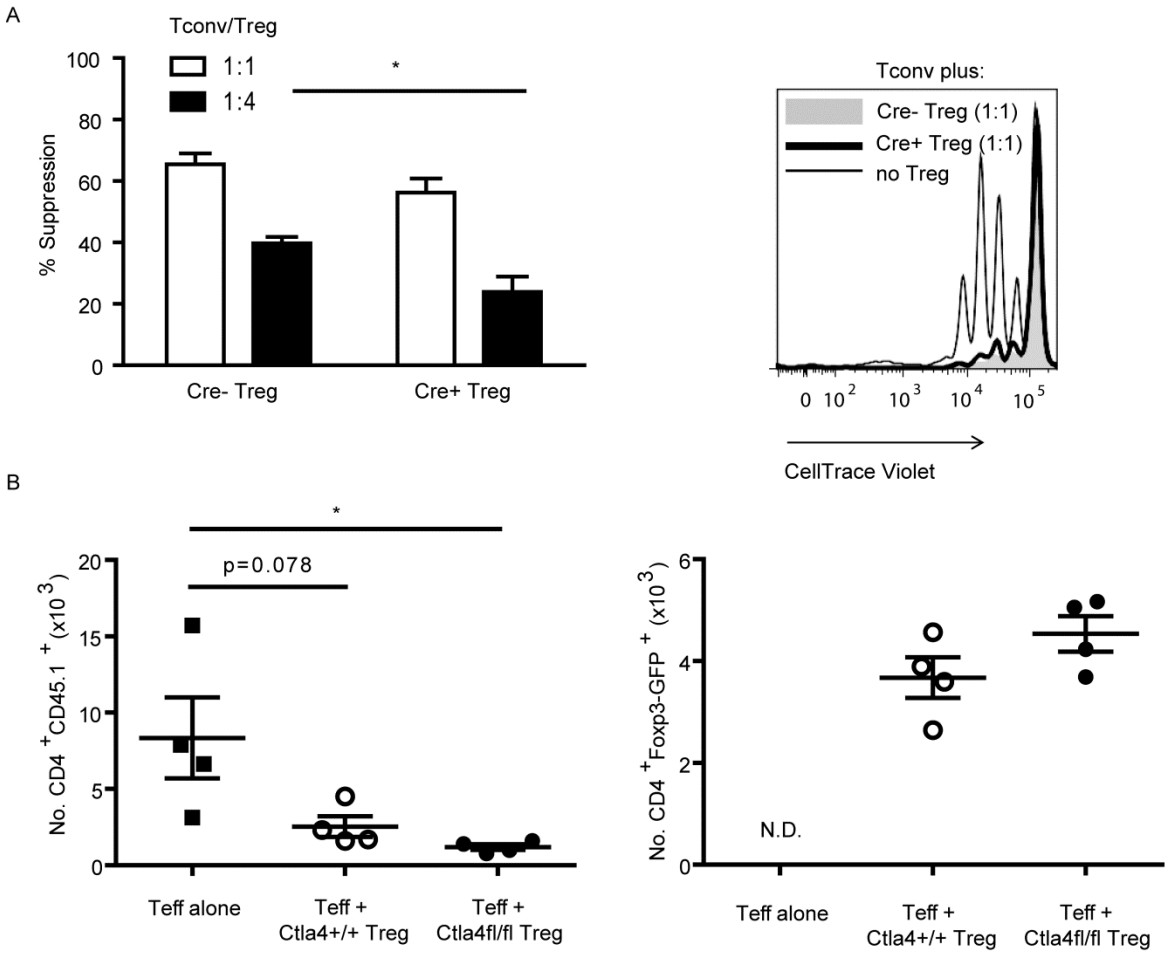
A
Tconv/Treg
1:1
1:4
*
% Suppression
100
80
60
40
20
0
Cre- Treg
Cre+ Treg
Tconv plus:
Cre- Treg (1:1)
Cre+ Treg (1:1)
no Treg
0 10^2 10^3 10^4 10^5
CellTrace Violet
B
*
p=0.078
No. CD4 +CD45.1 + (x10 3)
20
15
10
5
0
Teff alone
Teff + Ctla4+/+ Treg
Teff + Ctla4fl/fl Treg
No. CD4 +Foxp3-GFP + (x10 3)
6
4
2
0
N.D.
Teff alone
Teff + Ctla4+/+ Treg
Teff + Ctla4fl/fl Treg

Figure 5

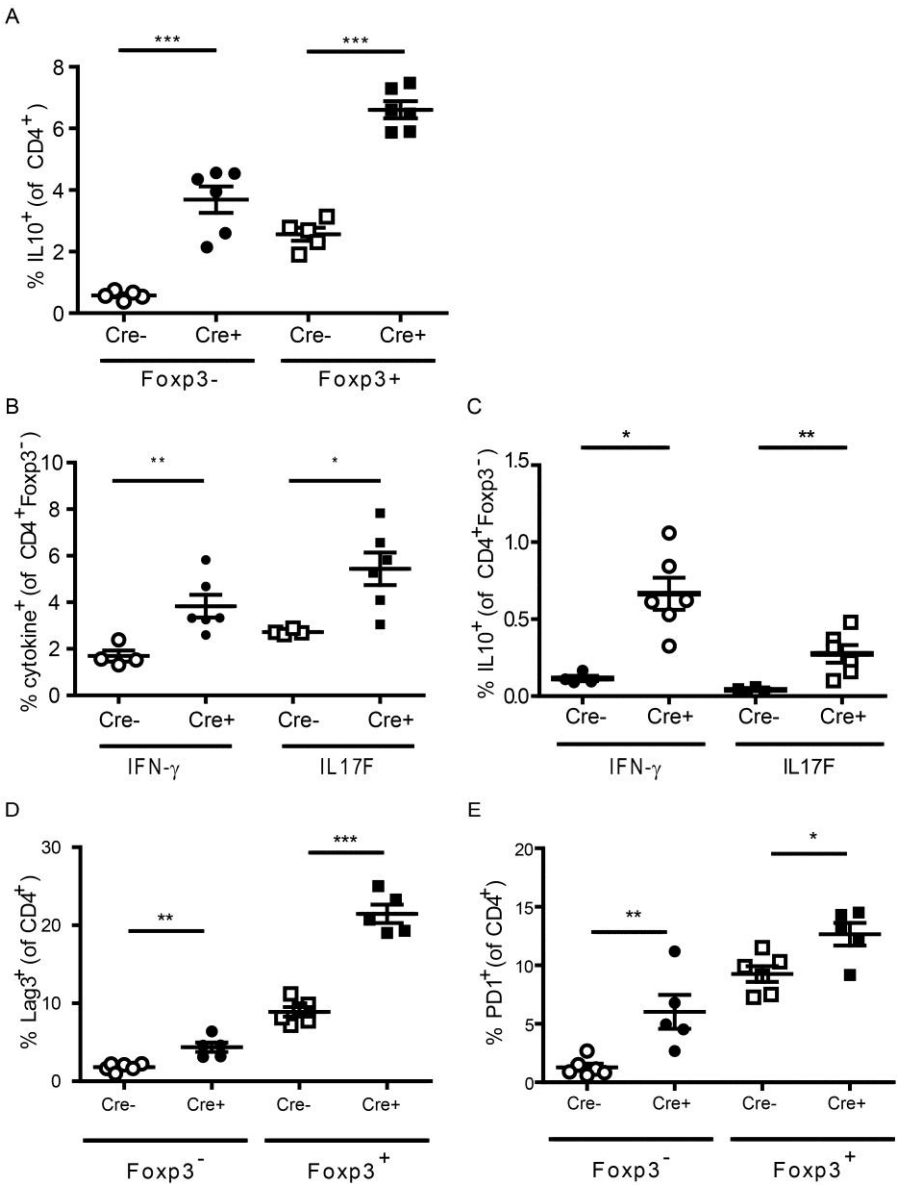
A
***
***
% IL10+ (of CD4+)
8
6
4
2
0
Cre-
Cre+
Cre-
Cre+
Foxp3-
Foxp3+
B
**
*
% cytokine+ (of CD4+Foxp3-)
10
8
6
4
2
0
Cre-
Cre+
Cre-
Cre+
IFN-γ
IL17F
C
*
**
% IL10+ (of CD4+Foxp3-)
1.5
1.0
0.5
0.0
Cre-
Cre+
Cre-
Cre+
IFN-γ
IL17F
D
**
***
% Lag3+ (of CD4+)
30
20
10
0
Cre-
Cre+
Cre-
Cre+
Foxp3-
Foxp3+
E
**
*
% PD1+ (of CD4+)
20
15
10
5
0
Cre-
Cre+
Cre-
Cre+
Foxp3-
Foxp3+

Figure 6

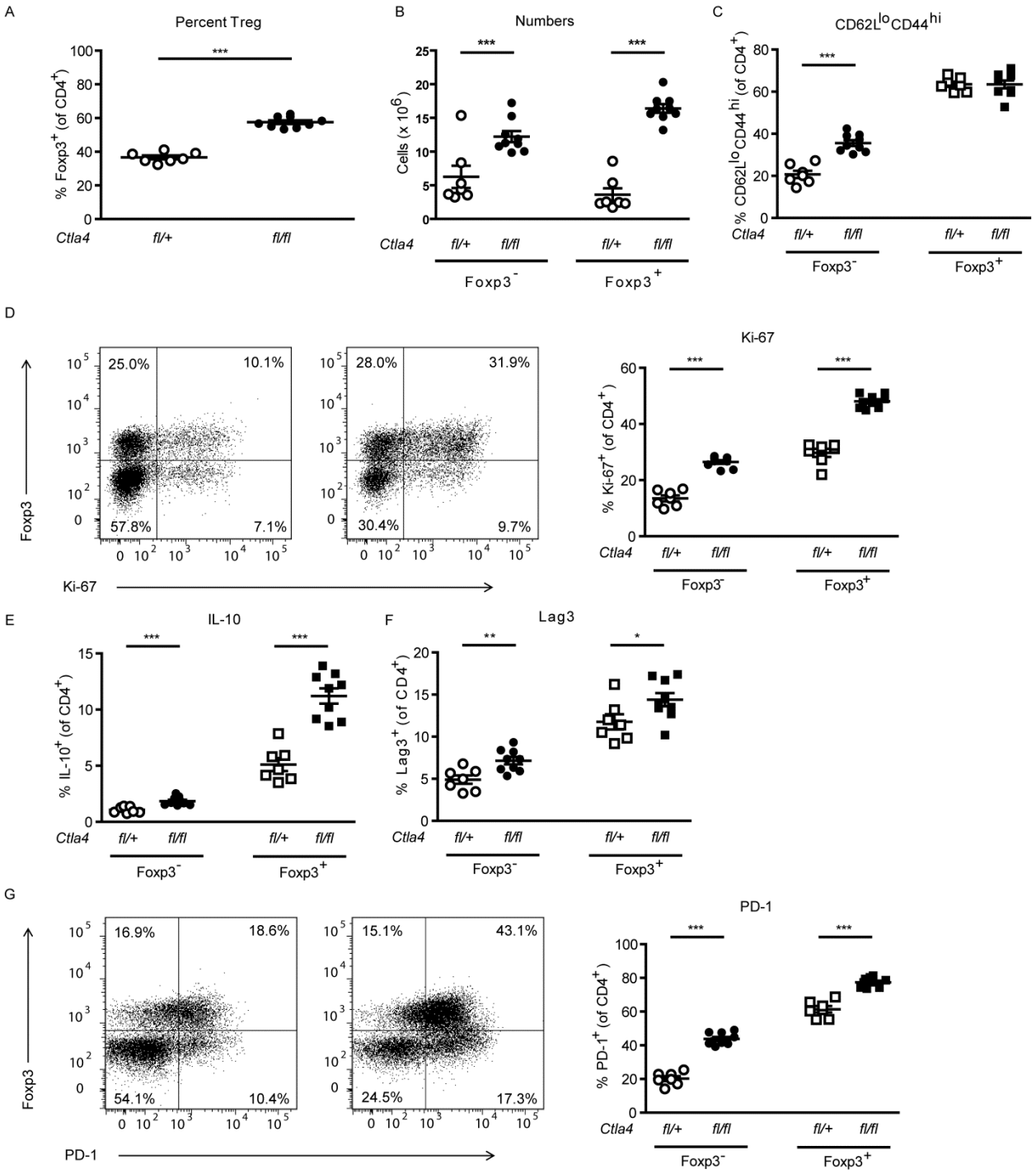
A
Percent Treg
% Foxp3+ (of CD4+)
Ctla4
fl/+
fl/fl
B
Numbers
Cells (x 10^6)
Foxp3-
Foxp3+
C
CD62LloCD44hi
% CD62LloCD44hi (of CD4+)
D
Foxp3
Ki-67
25.0%
10.1%
57.8%
7.1%
28.0%
31.9%
30.4%
9.7%
% Ki-67+ (of CD4+)
E
IL-10
% IL-10+ (of CD4+)
F
Lag3
% Lag3+ (of CD4+)
G
PD-1
16.9%
18.6%
54.1%
10.4%
15.1%
43.1%
24.5%
17.3%
% PD-1+ (of CD4+)

Figure 7

Supplemental Figure Legends

Figure S1. Targeting strategy and map of construct used to generate CTLA-4 conditional knockout mouse. Exons of the *Ctla4* gene are depicted by filled, numbered boxes. Exon 1: leader; Exon 2: IgV; Exon 3: transmembrane; Exon 4: cytoplasmic. Arrows indicate loxP sites.

Figure S2. Deletion of CTLA-4 on tamoxifen-treated *UBC$^{Cre/ERT2+}$Ctla4$^{fl/fl}$* mice.

Ctla4$^{fl/fl}$ mice that were either *UBC$^{Cre/ERT2-}$* (Cre^{-}) or *UBC$^{Cre/ERT2+}$* (Cre^{+}) were treated with tamoxifen, and RNA was isolated from splenocytes and analyzed for CTLA-4 expression by qPCR. Expression of Rpl13a was used as the normalization standard. Data are plotted as percent expression relative to Cre^{-} controls.

Figure S3. CTLA-4 deletion in adulthood does not induce autoimmunity. *Ctla4$^{fl/fl}$* mice that were either *UBC$^{Cre/ERT2-}$* (Cre^{-}) or *UBC$^{Cre/ERT2+}$* (Cre^{+}) were treated with tamoxifen at 8 weeks of age. At 6 months of age, mice were sacrificed, the indicated organs were harvested and fixed in formalin, and paraffin-embedded sections were stained with hematoxylin and eosin. All images are at 100x magnification.

Figure S4. Mice lacking CTLA-4 have reduced inflammatory foci in the CNS following EAE induction. *Ctla4*$^{fl/fl}$ mice that were either *UBC*$^{Cre/ERT2-}$ (Cre^{-}) or *UBC*$^{Cre/ERT2+}$ (Cre^{+}) were treated with tamoxifen and immunized with MOG_{35-55} to induce EAE. At day 30 post immunization, CNS pathology was assessed. Data are representative of at least three independent experiments.

Figure S5. Non-Treg deleted for Ctla4 are able to transfer EAE. Sorted CD4^{+}Foxp3-GFP^{-} T cells from either *UBC*$^{Cre/ERT2-}$ (Cre^{-}) or *UBC*$^{Cre/ERT2+}$ (Cre^{+}) mice were transferred to TCR$\alpha^{-/-}$ recipients that were immediately treated with tamoxifen for 5 consecutive days. Seven days after the transfer, mice were immunized with MOG_{35-55} to induce EAE, and monitored for disease development. n ≥ 7 mice per group

Figure S6. Transcriptional analysis of CTLA-4 deleted Tconv and Treg. *Ctla4*$^{fl/fl}$ mice that were either *UBC*$^{Cre/ERT2-}$ (Cre^{-}) or *UBC*$^{Cre/ERT2+}$ (Cre^{+}) were treated with tamoxifen and immunized with MOG_{35-55} to induce EAE. At the peak of disease, mice were sacrificed and Tconv and Treg cells were isolated from cervical lymph nodes by cell sorting. RNA was isolated as described, and gene expression quantified by NanoString analysis. Each column represents an individual mouse (3 mice per group).

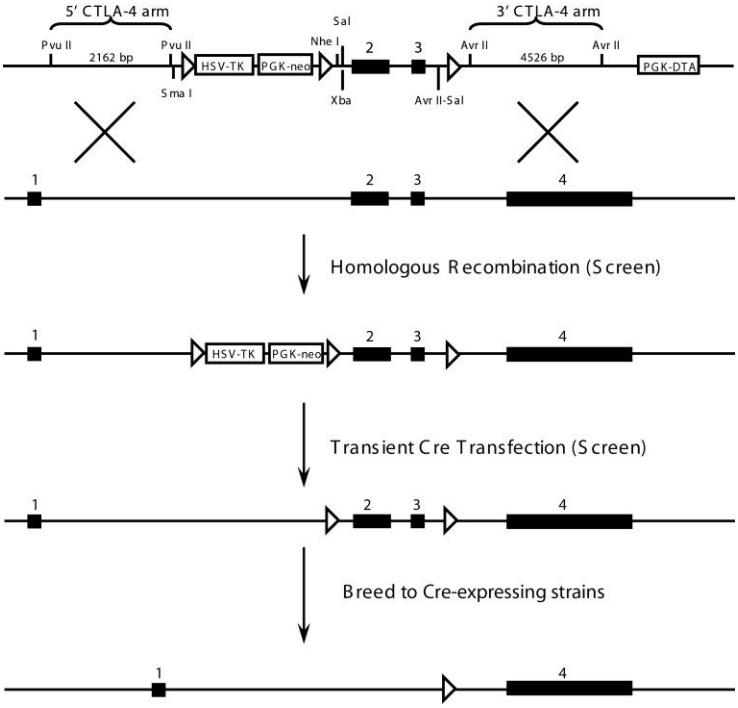

Supplemental Figure 1

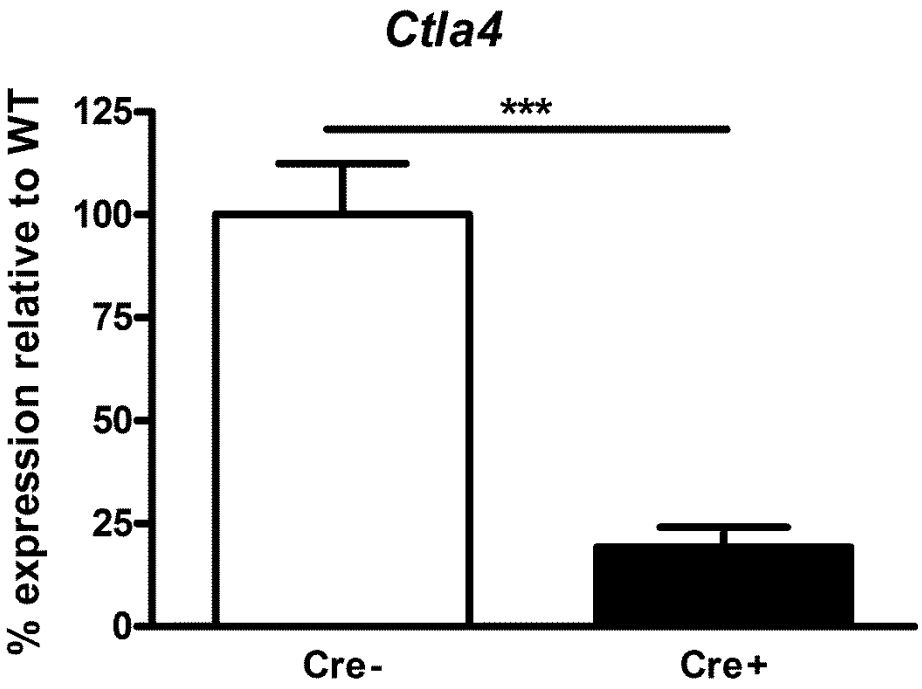

Supplemental Figure 2

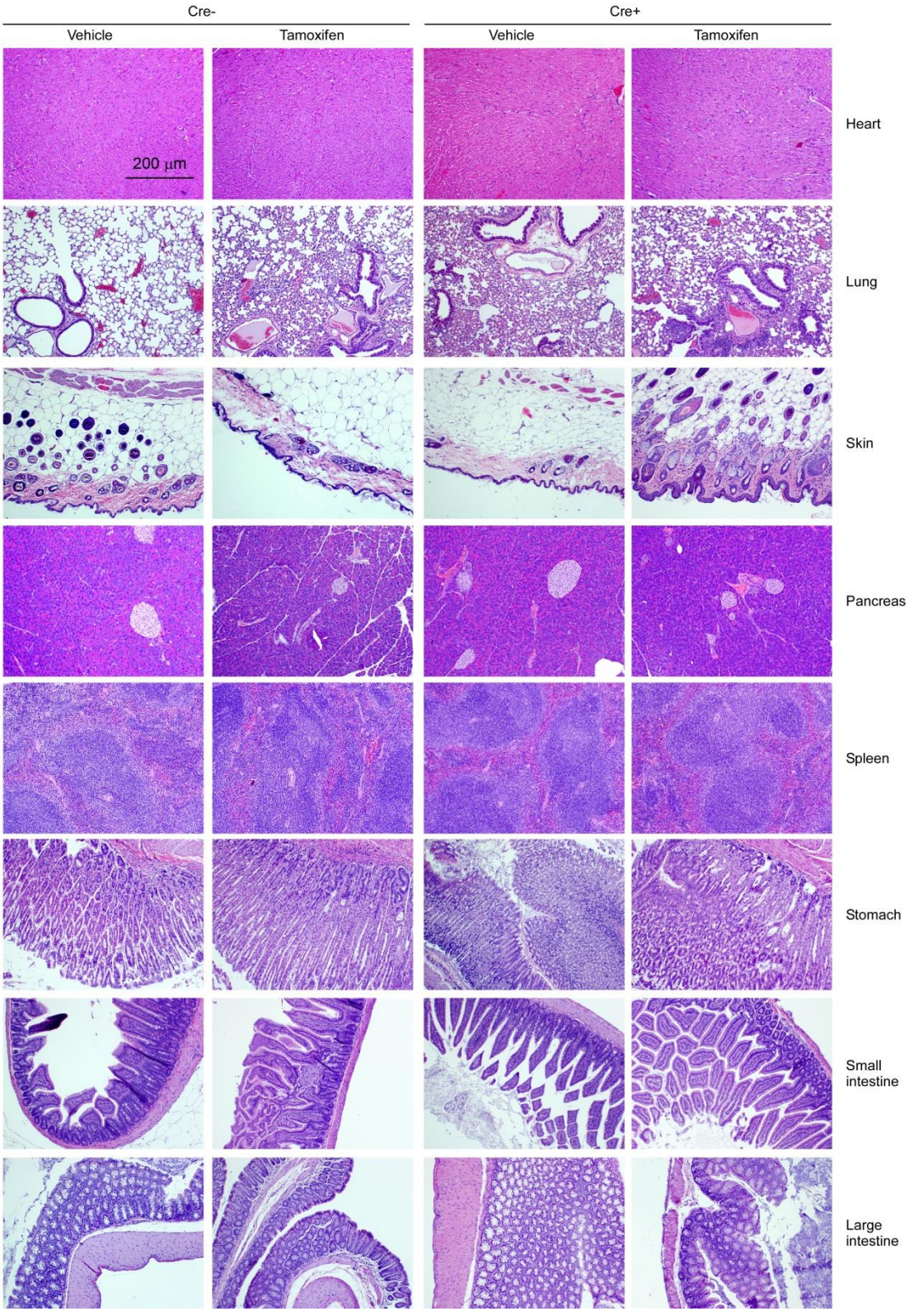

Supplemental Figure 3

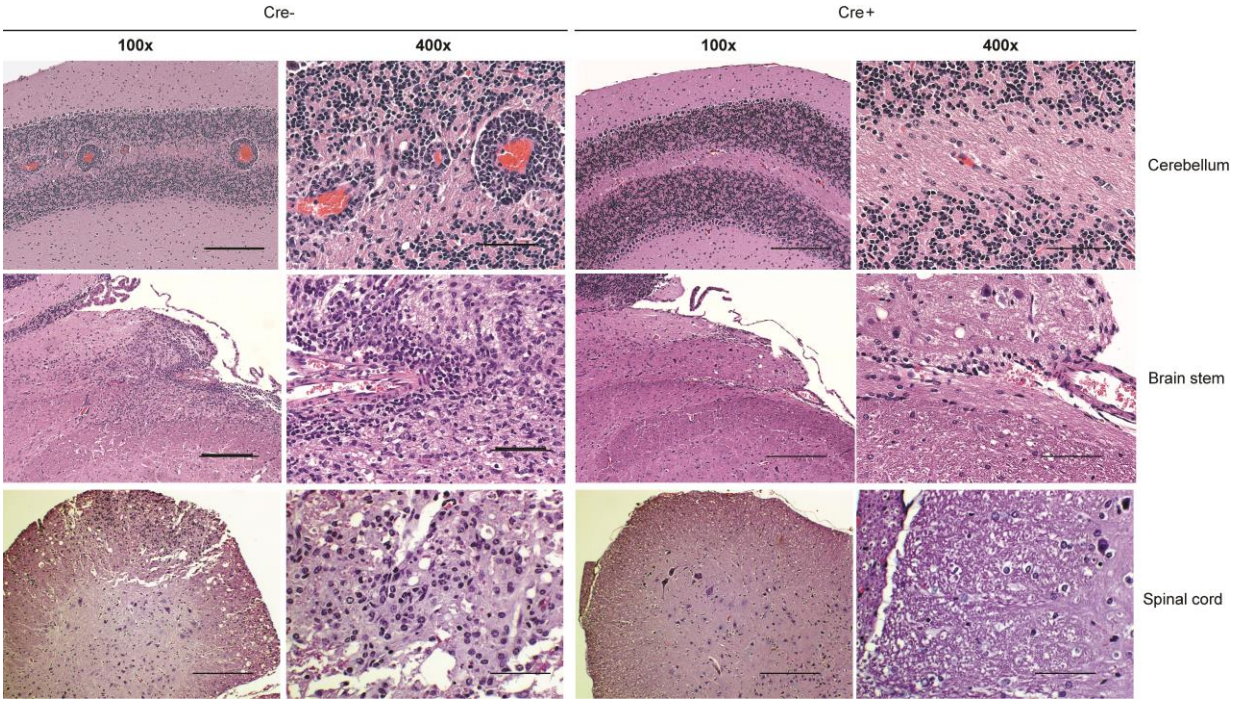

Supplemental Figure 4

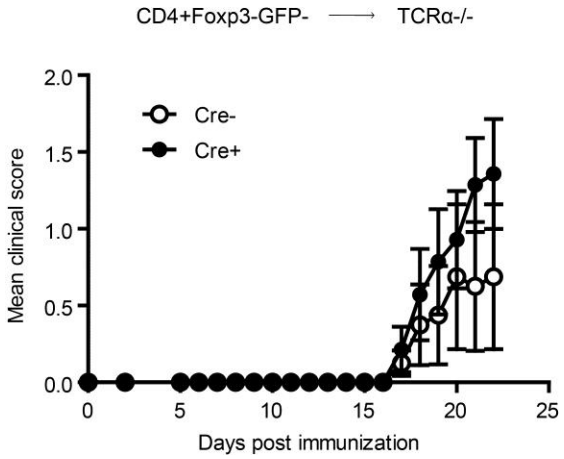

Supplemental Figure 5

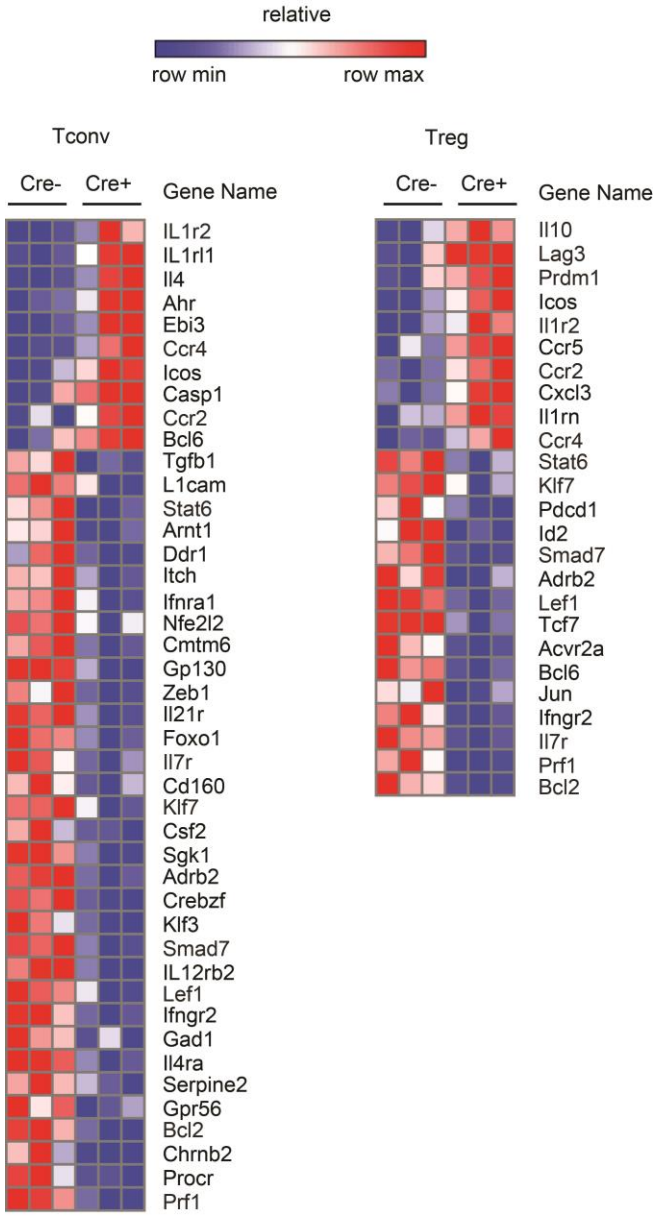

Supplemental Figure 6

Suppressive TFR cells Contribute to Defective Antibody Production in Aging

Peter T. Sage[1], Catherine Tan[1], Gordon J. Freeman[2], Marcia Haigis[3] and Arlene H. Sharpe[1,4]*

[1]Department of Microbiology and Immunobiology, Harvard Medical School, Boston, MA, 02115
[2]Department of Medical Oncology, Dana-Farber Cancer Institute, Department of Medicine, Harvard Medical School, Boston, MA, 02115
[3]Department of Cell Biology, Harvard Medical School, Boston, MA, 02115
[4]Department of Pathology, Brigham and Women's Hospital, Boston, MA, 02115

*Correspondence: Arlene_Sharpe@hms.harvard.edu

Running Title: TFR cells in Aging

Current character count= 30,294

Abstract

Defective antibody production in aging is broadly attributed to immunosenescence, however the precise immunological mechanisms are still not understood. Here we demonstrate increases in both T follicular helper (TFH) and T follicular regulatory (TFR) cells in aged mice, with an overrepresentation of TFR cells compared to TFH cells. Aged TFH and TFR cells in aged mice are phenotypically distinct from those in young mice, exhibiting increased PD-1 expression but decreased ICOS expression. Surprisingly, we find that aged TFH cells are not globally defective, but instead are dysfunctional in responding to specific antigen. PD-L1 blockade can rescue TFH cell function. In contrast, young and aged TFR cells have similar suppressive capacity on a per cell basis in antigen-specific suppression assays. Together these studies reveal a novel mechanism contributing to defective humoral immunity in aging: the increase in suppressive TFR cells in aged mice combined with impaired function of antigen-specific aged TFH cells results in reduced T cell dependent antibody responses.

Introduction

It has been widely observed that the extent of humoral immunity, or immunity provided by antibodies, decreases with age in both mice and humans (Goidl et al., 1976; Phair et al., 1978). This decrease in humoral immunity within the elderly population translates into increases in both the frequency and severity of infectious diseases in aged individuals (Goronzy and Weyand, 2013). Furthermore, vaccination of the elderly provides inadequate protection against most infectious diseases, leaving these individuals vulnerable to a number of diseases (Sasaki et al., 2011; Goronzy and Weyand, 2013). In contrast, vaccination of children and young adults provides effective protection.

The production of high affinity antibodies results from a complex interaction of B cells with T follicular helper (T_{FH}) cells in the germinal center reaction. T_{FH} cells are a subset of $CD4^+$ T cells that are uniquely specialized to help B cells. After differentiation, $CXCR5^+$ T_{FH} cells migrate to the B cell follicle via gradients of CXCL13 and provide help to B cells via costimulation (through ICOS and CD40L), as well as cytokine production (via IL-21 and IL-4)(Breitfeld et al., 2000; Crotty, 2011). Mice lacking T_{FH} cells, or their key effector molecules, have severely defective antibody production in response to T dependent antigens.

T follicular regulatory (T_{FR}) cells are a recently defined specialized subset of effector Tregs that inhibit antibody production (Chung et al., 2011; Linterman et al., 2011; Sage et al., 2013; Wollenberg et al., 2011). T_{FR} cells originate from natural Tregs (Chung et al., 2011; Sage et al., 2013) in contrast to T_{FH} cells which develop from naïve $CD4^+$ T cell precursors. Similarly to T_{FH} cells, T_{FR} cells express CXCR5, ICOS and PD-1, as well as the transcription factor Bcl6. PD-1 expression on T_{FR} cells limits both the

differentiation and effector function of TFR cells (Sage et al., 2013). TFR cells suppress antibody production potently in vitro and in vivo, but how they exert these suppressive effects is not yet clear. We have demonstrated that the TFH/TFR ratio is an important factor in humoral immunity that dictates the magnitude of antibody responses(Sage et al., 2013). Therefore, successful humoral immunity is a delicate balance between stimulatory TFH cells and inhibitory TFR cells, and not simply a result of a total number of TFH cells. Importantly, TFR cells are specialized in their suppression of antibody production as non-TFR Tregs do not have similar suppressive capabilities in vivo (Sage et al., 2013). Therefore, the immune system has evolved specialized mechanisms to both stimulate and suppress B cell responses.

The precise mechanisms leading to poor B cell responses in the aged are not understood. In 1969, Walford used the term immunosenescence to describe the decline in the immune system with age(Walford, 1969). In the T cell compartment, thymic involution, leading to reduction in the output of naïve T cells in the elderly, is one hypothesized cause of immune system decline (Scollay et al., 1980). Reduced naïve cell output is similar for the B cell compartment in the bone marrow (Miller and Allman, 2003). Beyond a decrease in generation of naïve lymphocytes (and in increase in memory cells), there are also alterations in the ability of naïve lymphocytes to become activated and form memory cells (Haynes et al., 2003; Linton and Dorshkind, 2004). Some, but not all, of these alterations can be rescued with addition of IL-2, since IL-2 production is attenuated with age (Haynes et al., 1999). Although decreased immune responses are largely attributed to defects in naïve cell populations, there are also increased numbers of natural Tregs in lymphoid organs (but not the blood) (Jagger et al.,

2014). It is not yet clear if Tregs from aged individuals are equally or more suppressive compared to Tregs from younger individuals (Nishioka et al., 2006; Raynor et al., 2012). This ambiguity results, at least in part, from the mixture of different naïve and effector Treg subsets in vivo that may respond differently during aging. Despite a number of studies that analyze the total $CD4^+$ T cell and Treg populations in the aged, it is still unclear if alterations exist in TFH and TFR cells. A previous study found no difference in $CXCR5^+$ cells in aged mice, however TFR cells were not assessed (Eaton et al., 2004). Understanding changes in these cells during aging is important because TFH and TFR cells directly interact with cognate B cells and function to control antibody production.

In this study we compared TFH and TFR cell development and function in young and aged mice. We find increases in both TFH and TFR cells in aged mice, however TFR cells predominate. We additionally show that TFH cells from aged mice are able to support antibody production, but they are defective in antigen-specific B cell stimulation. Aged and young TFR cells, however, have comparable suppressive capacity. Thus, our studies reveal a new mechanism to explain defective antibody responses in the aged: The over-abundance of highly suppressive TFR cells in aged mice, together with the inability of TFH cells to fully respond to specific antigen, results in an overall decrease in B cell responses.

Results and Discussion

Increased TFR Polarization in Aged Mice

To determine if altered TFH and TFR cells contribute to defective antibody production in aged mice, we first compared antibody production in 2 month old (young) and 20 month

old (aged) C57Bl/6 mice 10 days after subcutaneous (s.c.) immunization with NP-OVA in CFA, which promotes antibody production as well as TFH and TFR cell development and function (Sage et al., 2013). We found that aged mice had greater total serum IgM and IgG titers than young mice, however NP-specific IgG (but not IgM) antibody titers were significantly lower (**Fig. 1a**). Therefore, aged mice produce less antigen-specific antibody following immunization.

To understand the defect in antigen-specific antibody production in aged mice, we next determined if TFH and/or TFR cells were altered in aged mice. First, we compared TFH and TFR cells in the basal state (without immunization) in young and aged mice. TFH cells, defined as $CD4^+ICOS^+CXCR5^+FoxP3^-CD19^-$ cells were low in percentage in the inguinal lymph node and blood of both unimmunized young and aged mice, with slightly higher TFH cells in the blood of aged mice compared to young mice (**Fig 1b**). The increased TFH cells in the blood of aged mice are likely to be memory cells, since we have shown that blood TFH and TFR cells have characteristics of memory cells ((Sage et al., 2013; and manuscript submitted). TFR cells, defined as $CD4^+ICOS^+CXCR5^+FoxP3^+CD19^-$ cells were also low in percentage in the inguinal lymph node and blood of both unimmunized young and aged mice (**Fig 1c**).

Next, we compared the generation of TFH and TFR cells in young and aged mice upon antigenic challenge. We immunized young and aged mice with NP-OVA s.c. and measured TFH and TFR cell percentages in the draining lymph node (dLN) and blood 7 days later. TFH cells increased 3-fold by percentage in the dLN of aged mice compared to young mice after immunization (**Fig. 1d-e**). Increased TFH percentages were also found in the blood and spleen. TFR cells also increased sharply in the dLNs, blood and spleen of

immunized aged mice compared to young mice (**Fig. 1d,f**). We have previously demonstrated that the TFR:TFH ratio, or the proportion of $CXCR5^+$ cells in or capable of entering the germinal center that are $FoxP3^+$, predicts suppression of immune responses (Sage et al., 2013). To assess this in aged mice, we calculated TFR cells as a percentage of total $CD4^+CXCR5^+$ cells. In the dLN, there was a marked overrepresentation of TFR cells in the $CXCR5^+$ $CD4^+$ T cell pool, but this was not seen in the blood or spleen (**Fig. 1g**). The increase in TFR percentages of the total $CD4^+CXCR5^+$ pool is partially due to increased total Tregs (which are TFR precursors) in aged mice (**Fig. 1h**). These data indicate in response to an antigenic stimulus, there is an accumulation of TFR cells that increases the TFR:TFH ratio in dLN, which may account for defective antibody production in aged mice.

Aged TFR cells express more PD-1 and less ICOS and accumulate in Peyer's Patches

Next we determined if aged TFH and TFR cells were phenotypically distinct from young TFH and TFR cells, and not just increased in proportion in $CD4^+FoxP3^-$ and $CD4^+FoxP3^+$ cell populations, respectively. We previously determined that PD-1 suppresses both the differentiation and effector function of TFR cells (Sage et al., 2013). Therefore, we compared PD-1 expression on TFR and TFH cells from young and aged mice immunized with NP-OVA. We found substantial increases in the level of PD-1 expression on both TFR and TFH cells in aged mice (**Fig. 2a**). Greater PD-1 expression may inhibit TFR (and TFH) differentiation, function and maintenance. Increased PD-1 expression was not unique to TFH and TFR cells in aged mice, as $CD4^+CXCR5^-$ cells (a gate comprised mostly of naïve cells) also had slightly elevated PD-1 expression.

The costimulatory molecule ICOS is essential both for the differentiation of TFR cells and the differentiation/maintenance of TFH cells. Therefore, we compared ICOS expression levels on TFR and TFH cells from young and aged immunized mice. We found that TFH cells from the dLN had lower ICOS expression in aged mice compared to young mice (**Fig. 2b**). Additionally, TFR cells from the dLN had much lower expression of ICOS in aged mice, compared to young mice. Decreased ICOS expression may impact the functionality of both TFH and TFR cells. This phenotype was unique to TFH and TFR cells, as we did not detect differences in ICOS expression on $CD4^+CXCR5^-FoxP3^-$ cells or $CD4^+CXCR5^-FoxP3^+$ cells from the dLN after immunization.

Bcl6 is thought to be the master transcription factor for TFH cells, and is essential for TFR cell differentiation (Linterman et al., 2011; Nurieva et al., 2009). Bcl6 is also an oncogene frequently activated in non-hodgkins lymphoma, and expression of Bcl6 can inhibit cellular senescence (Shvarts et al., 2002). When we measured Bcl6 expression in TFH and TFR cells, we found no measurable differences between young and aged TFH and TFR cells, demonstrating that altered Bcl6 expression in TFH and TFR cells is not responsible for increased TFH and TFR expansion in immunized aged mice (**Fig. 2c**). However, both $CD4^+CXCR5^-FoxP3^-$ and $CD4^+CXCR5^-FoxP3^+$ populations in aged mice had significantly higher levels of Bcl6 compared to young mice, suggesting that higher Bcl6 expression in TFR and TFH precursor cells may lead to increased differentiation and result in increased TFR and TFH percentages in immunized aged mice.

Next we assessed cell death due to previous reports that aged Tregs had decreased expression of the proapoptotic molecule BIM, which may lead to enhanced Treg survival (Chougnet et al., 2011). Inhibition of cell death is one potential explanation for increases

in TFR cells in the aged mice. However, cell death, as measured by active caspase staining with VAD-FMK was unchanged between young and aged TFH and TFR cells (**Fig. 2d**). Cell activation, measured by expression of the cell cycle marker Ki67, was significantly reduced; there were lower percentages of TFR and TFH cells in cell cycle in aged mice compared to young mice (**Fig. 2e**). Therefore, increased cell cycling is not the reason for the greater percentages of TFR or TFH cells in aged mice. The increased Bcl6 expression on TFH and TFR precursors in aged mice, combined with the lack of significant differences in cell death and lower cell cycling, led us to hypothesize that over-representation of TFR cells in aged mice may due to increased TFR cell generation and not maintenance.

Since FoxP3 expression levels may control Treg suppression and stability (Sakaguchi et al., 2013; Williams and Rudensky, 2007), we also compared FoxP3 expression in TFR cells from young and aged mice. TFR cells (as well as total Tregs) from immunized aged mice had slightly attenuated FoxP3 levels compared to young mice (**Fig. 2e**), suggesting that TFR cells in aged mice may have defective suppressive capacity. Taken together, these data indicate that TFR cells in aged mice are phenotypically distinct from TFR cells in young mice and have increased PD-1, but attenuated ICOS and FoxP3 expression which may alter their effector functions and/or their stability.

Besides lymph nodes and blood, TFH cells can also reside in peyer's patches (PP) of the gut where they enhance IgA production (Tsuji et al., 2009). This led us to compare TFH cells in PP of young and aged mice, and determine if TFR cells were present in PP. The cues for TFH cell differentiation and persistence in the PP are thought to be supplied constantly by the gut microbiota. We found a substantial population of TFH cells in PP of

unimmunized young mice, but the percentage of these cells was indistinguishable from aged mice (**Fig 2g** and data not shown). It is not currently known if TFR cells reside within the PP, however previously reported decreased IgA production in aged individuals might be due to TFR cells. When we analyzed TFR cells in the PP, we found a substantial population in the PP of both young and aged mice (**Fig 2g**). Since we found that the TFR population is proportionally increased compared to TFH cells in LN of immunized aged mice, we assessed the percentage of TFR cells of $CXCR5^+$ cells in the PP. We found that there was a larger contribution of TFR cells to the total $CXCR5^+$ $CD4^+$ T cell pool in PP of aged mice compared to young mice (**Fig 2g**). This overrepresentation of TFR cells in PP may lead to lower IgA production and contribute to a change in microbiota in the gut in aged animals.

ICOS expression was also significantly attenuated on TFR cells, but not TFH cells, in the PP of aged mice, suggesting that decreased ICOS expression on TFR cells is a general phenotype of TFR cells in aged mice in a number of anatomical locations (**Fig. 2h**). FoxP3 expression in PP however, was similar in aged and young TFR cells, which contrasts to the lower FoxP3 expression seen in LN TFR cells from aged mice compared to young mice (**Fig. 2i**). Taken together, these studies indicate that TFR are proportionally increased in PP as well as LN cells of aged mice, and this increase may alter T cell dependent antibody production in aged mice.

Aged TFH cells Have Less Antigen-specific Stimulatory Capacity

We next investigated TFH cell function in aged mice since immunosenescence has been postulated to cause cell-intrinsic defects in effector cells in aging. It is important to

separately analyze aged TFH cells and TFR cells because functional changes in both populations may contribute to defective antibody production in aged mice. Therefore, we compared the stimulatory capacity of purified young and aged TFH cells to determine if aged TFH cells have cell-intrinsic defects in their ability to stimulate B cells. We first used antigen-non-specific in vitro B cell class switch recombination assays that we developed (manuscript submitted and (Sage et al., 2013)). In these assays, TFH cells were sorted (sorted as $CD4^+ICOS^+CXCR5^+GITR^-CD19^-$) from dLNs of young (2 month) or aged (20 month) mice that were immunized with NP-OVA s.c. 7 days previously. These TFH cells were cultured with young $CD19^+$ B cells (isolated from dLNs of similarly immunized mice) along with anti-IgM and anti-CD3. These assays sensitively assess cell-intrinsic TFH effector function separately from TFH differentiation and do not depend on the antigen specificity of the TFH cell. Surprisingly, we found that young and aged TFH cells similarly stimulated B cells to class switch to IgG1 and, therefore, there was no evidence of altered intrinsic function in the TFH cell compartment of aged mice (**Fig. 3a**). Without the addition of TFH cells, B cells expressed little IgG1 demonstrating the strong stimulatory capacity of young and aged TFH cells. We next examined expression of the germinal center and activation marker GL7 on B cells because we have found that GL7 expression is a sensitive marker for B cell activation in these assays. GL7 was similarly upregulated on B cells when either young or aged TFH cells were in the cultures (**Fig 3a**). Moreover, intracellular expression of Bcl6 and Ki67 were similar in young and aged TFH cells following culture with B cells (**Fig. 3b**). These unexpected findings suggest that the young and aged TFH cells have comparable stimulatory capacity in these in vitro antigen non-specific assays. Therefore, although numerous defects have

been demonstrated in the $CD4^+$ T cell compartment with advancing age, TFH cells from young and aged mice appear to have similar cell intrinsic capacity to participate in B cell help.

The similar stimulatory capacity of young and aged TFH cells was perplexing given the defective antibody production in immunized aged mice. Possibly, TFH cells from aged mice were functional, but not antigen specific. To test this hypothesis, we adapted the in vitro assays to assess antigen-specific responses. We cultured young B cells with young or aged TFH cells (all sorted from dLNs of NP-OVA immunized mice) along with NP-OVA for 6 days and measured B cell activation and class switch recombination. Young TFH cells elicited ~twice as much class switching to IgG1 in antigen-specific assays compared to antigen non-specific assays (**Fig. 3c**). When we compared young and aged TFH cells in these antigen specific assays, we found that aged TFH cells stimulated B cells to undergo IgG1 or IgG2a class switch recombination slightly less than young TFH cells (**Fig. 3c**). The activation marker GL7 was modestly attenuated when aged TFH cells were used in the cultures compared to young TFH cells (data not shown). A slightly lower percentage of aged TFH cells expressed Bcl6 and Ki67 expression compared to young TFH cells (**Fig. 3d**). Therefore, the aged TFH cells in antigen specific stimulation assays were slightly reduced, leading to modestly defective antibody production by the B cells in vitro.

Next we determined if aged TFH cells had less stimulatory capacity in vivo in the absence of aged TFR cells. To do this, we performed adoptive transfer experiments in which TFH cells from dLNs of NP-OVA immunized young or aged mice cells were adoptively transferred to young $CD28^{-/-}$ mice that were immunized with the same antigen.

$CD28^{-/-}$ recipients lack TFH and TFR cells, but have naïve $CD4^+$ T cells, preventing homeostatic proliferation, but allowing analyses of TFH cell function in vivo, as we have described previously (Sage et al., 2013). These in vivo TFH transfer experiments showed that aged TFH cells stimulated less GC B cell differentiation, plasma cell formation and NP-specific antibody production in vivo compared to young TFH cells (**Fig 3e-g**). The function of aged TFH cells to support B cell responses was impaired to a much greater extent in vivo compared to the modest defects seen in vitro. These differences in severity of TFH cell dysfunction are likely due to the increased requirement for proliferation during in vivo experiments compared to in vitro assays. Alternatively, it is possible that TFH and/or B cells have a higher threshold for activation in vivo than in our in vitro assays.

Since PD-1 is more highly expressed on aged TFH cells and PD-1 blockade has been shown to enhance $CD4^+$ T cell cytokine production and $CD8^+$ proliferation in aged mice (Lages et al., 2010; Mirza et al., 2010) we next determined whether PD-1 pathway blockade could overcome some of the age-related defects in TFH cell function. We analyzed the effects of a PD-L1 blocking antibody in the cultures of aged TFH cells with NP-OVA. An anti-PD-L1 blocking antibody was able to substantially enhance the stimulatory capacity of aged TFH cells in these antigen-specific B cell stimulation assays (**Fig 3h**). Taken together, these data indicate that aged TFH cells are not intrinsically defective, but instead show defects in activation following antigen-specific stimulation, and PD-L1 blockade can improve the function of antigen-specific TFH cells significantly. Thus, increased PD-1 expression on aged TFH may raise the threshold for activation of aged TFH in response to antigen.

Aged TFR cells Have Potent Suppressive Capacity

We next compared the suppressive function of young and aged TFR cells, since TFR cells predominate in aged mice, but appear to be phenotypically distinct from young TFR cells. First, we cultured young or aged dLN TFR cells with young dLN TFH and B cells using in vitro non-antigen-specific assays and stimulated the cells using anti-CD3 and anti-IgM, similarly to Fig. 3A. Both young and aged TFR cells were able to potently suppress class switch recombination to IgG1 under these conditions (**Fig 4a-b**). Young and aged TFR cells also were able to attenuate GL7 expression on B cells to almost levels of unstimulated B cells. We also investigated whether young TFH cells were suppressed to a similar degree as the B cells by young or aged TFR cells in these cultures. We assessed Ki67 expression to determine the percentage of TFH cells in cell cycle at the end of the culture. We found that young and aged TFR cells were comparable in their capacity to suppress Ki67 expression in TFH cells (**Fig 4c**). In addition, we compared the percentages of young versus aged TFR cells in cell cycle in these cultures and found that a similarly high proportion of young and aged TFR cells were in cell cycle (**Fig 4d**). Therefore, TFR cells from young and aged mice have similar and potent intrinsic suppressive capacity to inhibit B cell responses. Since TFR cells are greatly expanded in aged mice and these cells have suppressive capacity comparable to young TFR cells, these data indicate that the increase in TFR cells in aged mice is a major source of defective B cell responses.

Lastly, we analyzed TFR cell function using antigen-specific in vitro assays. We previously determined that young TFR cells do not need to be antigen specific to suppress B or TFH cells (manuscript submitted); however aged TFR cells may differ. We compared the suppressive capacity of young and aged TFR cells in OVA-specific TFH stimulation

assays. Aged and young TFR cells had virtually the same ability to suppress class switch recombination to IgG1 when NP-OVA was added to the cultures (**Fig 4e**). However, we did measure a significant decrease in the suppression of IgG2a by aged TFR cells compared to young TFR cells, albeit this was a minor difference of ~0.5% of the IgG2a (**Fig 4f**). When we examined Ki67 expression in the TFH cells, we found that there was no significant difference in the suppression of this cell cycle marker by young or aged TFR cells (**Fig 4g**). In addition, aged and young TFR cells similarly suppressed IFN-γ production by TFH cells (**Fig 4h**). We also found no significant difference in Ki67 expression by young or aged TFR cells at the end of the suppression assay (**Fig. 4i**). These data suggest that young and aged TFR cells have comparable suppressive function and are similarly reactivated.

Together, these results provide novel insights into mechanisms of defective antibody production in aging. We find an over-representation of functionally competent suppressive TFR cells in aged mice, most likely resulting from enhanced differentiation of TFR cells from FoxP3$^+$ CD4$^+$ regulatory T cells. We hypothesize that increased Bcl6 expression in the more numerous FoxP3$^+$ precursor cells overrides the potential inhibitory effects resulting from increased PD-1 expression and leads to an increase in the percentage of TFR cells. The marked increase in TFR cells, together with the decrease in antigen-specific responses of TFH cells, results in a substantial defect in antibody production in aged mice. Although other mechanisms such as defects in clonality and/or number of naïve B cells may also contribute, we hypothesize that the increase in TFR cells is one of the major causes of impaired antibody production in aging. Therefore,

modulation of TFR cells may provide a novel strategy for improving humoral immunity responses in the elderly.

Methods

Mice. Young mice were 8 week old C57Bl/6 mice and aged mice were 20 month old C57Bl/6 mice. Mice were obtained from the National Institute of Aging or Jackson Labs. *CD28*$^{-/-}$ mice (Shahinian et al., 1993) were purchased from The Jackson Laboratory. All mice were used according to the Harvard Medical School Standing Committee on Animals and National Institutes of Animal Healthcare Guidelines. Animal protocols were approved by the Harvard Medical School Standing Committee on Animals.

Immunizations. For standard NP-OVA immunizations, 100μg NP_{18}-OVA (Biosearch Technologies) in a 1:1 H37RA CFA (DIFCO) emulsion was injected subcutaneously in the flanks of young or aged mice. The inguinal lymph nodes (dLN), blood and spleen were harvested seven days later. Peyer's patches were harvested from unimmunized mice.

Flow Cytometry. Cells harvested from lymphoid organs were isolated and resuspended in staining buffer (PBS containing 1% fetal calf serum and 2mM EDTA) and stained with directly labeled antibodies from Biolegend against CD4 (RM4-5), ICOS (15F9), CD19 (6D5), IL-17A (TC11-18H10.1), IFNγ (XMG1.2), CD138 (281-2) and IgG2a (RMG2a-62), from eBioscience against FoxP3 (FJK-16S), Bcl6 (mGI191E), and from BD

Bioscience against GL7, Ki67 (B56) and IgG1 (A85-1). For CXCR5 staining, biotinylated anti-CXCR5 (2G8, BD Biosciences) was used followed by streptavidin-brilliant violet 421 (Biolegend). For intracellular staining of transcription factors and Ki67, the FoxP3 fix/perm kit was used (eBioscience) after surface staining was accomplished. For VAD-FMK staining the Caspglow kit was used according to manufacturer's instructions (eBioscience). For intracellular cytokine staining, cells were incubated with 1μg/ml ionomycin (Sigma) and 500ng/ml PMA (Sigma) in the presence of Golgistop (BD biosciences) for 4 hours prior to staining. All flow cytometry experiments were analyzed with an LSR II (BD biosciences) using standard filter sets. All cell sorting was performed on an Aria II cell sorter (BD biosciences) using a 70μm nozzle with 70psi pressure and the highest purity settings.

Adoptive Transfers. For young and aged TFH cell transfers, 10 young or 10 aged C57Bl/6 mice were immunized with NP-OVA subcutaneously as described above, and 7 days later dLN was harvested. $2x10^5$ $CD4^+ICOS^+CXCR5^+GITR^-CD19^-$ cells were sorted and adoptively transferred to *CD28*$^{-/-}$ mice that were then immunized subcutaneously with NP-OVA in CFA. 12 days later the draining lymph nodes and serum were harvested from mice. Draining lymph nodes were analyzed by flow cytometry. Serum was isolated from blood using serum separator tubes (BD vacutainer) and NP-specific IgG was measured by ELISA as previously described (Sage et al., 2013).

***In vitro* Suppression Assay.** After sorting, cells were counted on an Accuri cytometer (BD biosciences). For young and aged non-antigen specific TFH stimulation assays,

$3x10^4$ dLN $CD4^+ICOS^+CXCR5^+CD19^-GITR^-$ TFH cells from young or aged mice were plated with $5x10^4$ $CD19^+$ young B cells (all purified from dLNs of immunized with NP-OVA 7 days previously) and 2μg/ml soluble anti-CD3 (2C11, BioXcell) plus 5μg/ml anti-IgM (Jackson Immunoresearch) for 6 days. Cells were then harvested and stained for flow cytometry analyses. Antigen specific assays were performed in a similar way, except instead of anti-CD3 and anti-IgM, 20μg/ml NP-OVA was added to the cultures. In some experiments 20μg/ml of anti-PD-L1 (clone 9G2) or isotype control was added to the wells. For TFR cell suppression assays, $1.5x10^4$ $CD4^+ICOS^+CXCR5^+CD19^-GITR^+$ TFR cells from the dLN of young or aged mice immunized with NP-OVA 7 days previously were added to the wells of TFH cell non-antigen specific or antigen-specific assays. Cells were harvested and analyzed 6 days later.

Statistical Analysis. Unpaired Student's t test was used for all comparisons, data represented as mean +/- SD or SE are shown. P values < 0.05 were considered statistically significant. * $P<0.05$, ** $P<0.005$, *** $P<0.0005$.

Figure Legends

Figure 1. Increased TFR Cells in Aged Mice. (**a**) Comparison of antibody production in aged mice. 2 (young) or 20 (aged) month old C57Bl/6 mice were immunized subcutaneously (s.c.) with NP-OVA in CFA and 10 days later serum was collected and total IgM and IgG (top) or NP-specific IgM and IgG (bottom) were analyzed by ELISA. (**b-c**) Percentages of TFH and TFR cells in unimmunized young and aged mice. $CD4^+ICOS^+CXCR5^+FoxP3^-CD19^-$ TFH (top) and $CD4^+ICOS^+CXCR5^+FoxP3^+CD19^-$ TFR (bottom) were analyzed in young and aged mice. iLN = inguinal lymph node, (**d-f**) Representative plots (d) and quantification of TFH (e) and TFR (f) cells from the draining lymph nodes (dLNs) of young or aged mice 7 days after s.c. immunization. (**g**) Quantification of the TFR contribution to total $CD4^+CXCR5^+$ cells in the dLN of young and aged mice after immunization. (**h**) Quantification of total $FoxP3^+$ cells in the dLN of young or aged mice immunized with NP-OVA.

Figure 2. Aged TFR cells express more PD-1, less ICOS, and accumulate in Peyer's patches. (**a**) Comparison of PD-1 expression on young and aged TFR cells. $CD4^+ICOS^-CXCR5^-$ (CXCR5-), $CD4^+ICOS^+CXCR5^+FoxP3^-CD19^-$ (TFH) and $CD4^+ICOS^+CXCR5^+FoxP3^+CD19^-$ (TFR) cells from the dLN of 2 (young) or 20 (aged) month old mice immunized with NP-OVA s.c. 7 days previously were analyzed for PD-1 expression. Solid histogram indicates $CXCR5^-$ population. (**b**) Comparison of ICOS expression on young and aged TFR cells. $CD4^+CXCR5^-FoxP3^-CD19^-$ (FoxP3-CXCR5-), $CD4^+CXCR5^-FoxP3^+CD19^-$ (FoxP3+CXCR5-), $CD4^+CXCR5^+FoxP3^-CD19^-$ (TFH) and $CD4^+CXCR5^+FoxP3^+CD19^-$ (TFR) cells from dLNs of mice immunized as in (a) were

analyzed for ICOS expression. Representative histograms (left) and quantification (right) are shown. (**c**) Comparison of intracellular Bcl6 expression in young and aged TFR and TFH cells. Populations as in (b) were intracellularly stained for Bcl6. (**d**) Comparison of cell death in aged TFR and TFH cells assessed by activated caspase staining. Populations as in (a) were stained with active caspase binding reagent VAD-FMK. (**e**) Comparison of cell cycling in young and aged TFR and TFH cells. Populations as in (a) were intracellularly stained with anti-Ki67 to measure populations that are in cell cycle. Gating strategy (left) and quantification (right) are shown. (**f**) Comparison of FoxP3 expression in TFR cells from dLNs of young or aged immunized mice. (**g**) TFR and TFH cells in PP. Flow cytometric analysis of total $ICOS^+CXCR5^+$ cells in unimmunized young and aged mice (left) and quantification of TFR cells as a percentage of $ICOS^+CXCR5^+$ cells (right). (**h**) Comparison of ICOS expression on young and aged TFR cells from PP. Populations as in (b) were analyzed for ICOS expression. (**i**) Comparison of FoxP3 expression in TFR cells from PP of young or aged mice.

Figure 3. Aged TFH cells have defective antigen specific-antibody stimulatory capacity. (**a**) Non-antigen specific antibody stimulation assays. $CD4^+ICOS^+CXCR5^+GITR^-CD19^-$ (TFH) cells sorted from 10 pooled 2 (young) or 20 (aged) month old mice immunized with NP-OVA subcutaneously 7 days previously were plated with $CD19^+$ B cells from dLN of immunized young mice along with anti-CD3 and anti-IgM for 6 days. B cells were surface stained for GL7 and intracellularly stained for IgG1. Representative plots (left) and quantification (right) are pre-gated on $CD19^+IA^+$ B cells. (**b**) Ki67 and Bcl6 staining of young or aged TFH cells from assays as in (a). (**c**) Antigen-specific antibody

stimulation assays. $CD4^+ICOS^+CXCR5^+GITR^-CD19^-$ (T_{FH}) cells sorted from 2 (young) or 20 (aged) month old mice immunized with NP-OVA subcutaneously 7 days previously were plated with $CD19^+$ B cells from dLN of NP-OVA immunized young mice along with NP-OVA for 6 days. B cells were surface stained for GL7 and intracellularly stained for IgG1 or IgG2a. (**d**) Ki67 and Bcl6 staining of young or aged T_{FH} cells from assays as in (c). (**e-f**) Comparison of young and aged T_{FH} cell mediated B cell activation in vivo. Young or aged T_{FH} cells were sorted from NP-OVA immunized mice and adoptively transferred to $CD28^{-/-}$ recipients that were immunized with NP-OVA. 10 days later the draining lymph nodes were harvested and germinal center B cells (e) or plasma cells (f) were quantified. (**g**) NP-specific antibody titers were measured by ELISA. (**h**) Anti-PD-L1 blocking antibody can enhance the stimulatory capacity of aged T_{FH} cells. Aged T_{FH} cells were cultured with young B cells and NP-OVA as in (c) in the presence of αPD-L1 or isotype control. 6 days later B cells were quantified for class switch to IgG1.

Figure 4. Aged T_{FR} cells potently suppress T_{FH} mediated antibody production. (**a**) T_{FR} antigen non-specific suppression assays. Young or aged T_{FR} cells were cultured with young B cells and young T_{FH} cells (all from the dLN NP-OVA immunized mice) in the presence of anti-CD3 and anti-IgM. 6 days later B cells were surface stained for GL7 and intracellularly stained for IgG1. Representative plots are shown. (**b**) Quantification of $IgG1^+GL7^+$ cells in plots in (a). (**c**) Intracellular Ki67 staining on $FoxP3^-T_{FH}$ cells from cultures described in (a). (**d**) Intracellular Ki67 staining on $FoxP3^+T_{FR}$ cells from cultures described in (a). (**e**) Aged T_{FR} cells potently suppress antibody formation in antigen specific suppression assays. Sorted $CD4^+ICOS^+CXCR5^+GITR^+CD19^-$ (T_{FR}) cells

from 2 (young) or 20 (aged) month old mice immunized with NP-OVA subcutaneously 7 days previously were cultured with TFH and B cells from NP-OVA immunized young mice in the presence of NP-OVA. 6 days later B cells were stained for surface GL7 or intracellular IgG1. B cells were identified as $CD19^{+}IA^{+}$. (**f**) Intracellular staining of IgG2a in $CD19^{+}IA^{+}$ B cells from experiments as in (e). (**g**) Intracellular Ki67 staining on $CD4^{+}FoxP3^{-}$ TFH cells from cultures as in (e). (**h**) Intracellular staining of IFNγ and IL17A in TFH cells from cultures as in (e) after PMA/ionomycin stimulation for 4 hours. (**i**) Intracellular staining of Ki67 in young or aged TFR cells from cultures as in (e).

References

Breitfeld, D., L. Ohl, E. Kremmer, J. Ellwart, F. Sallusto, M. Lipp, and R. Forster. 2000. Follicular B helper T cells express CXC chemokine receptor 5, localize to B cell follicles, and support immunoglobulin production. *J Exp Med* 192:1545-1552.

Chougnet, C.A., P. Tripathi, C.S. Lages, J. Raynor, A. Sholl, P. Fink, D.R. Plas, and D.A. Hildeman. 2011. A major role for Bim in regulatory T cell homeostasis. *J Immunol* 186:156-163.

Chung, Y., S. Tanaka, F. Chu, R.I. Nurieva, G.J. Martinez, S. Rawal, Y.H. Wang, H. Lim, J.M. Reynolds, X.H. Zhou, H.M. Fan, Z.M. Liu, S.S. Neelapu, and C. Dong. 2011. Follicular regulatory T cells expressing Foxp3 and Bcl-6 suppress germinal center reactions. *Nat Med* 17:983-988.

Crotty, S. 2011. Follicular helper CD4 T cells (TFH). *Annu Rev Immunol* 29:621-663.

Eaton, S.M., E.M. Burns, K. Kusser, T.D. Randall, and L. Haynes. 2004. Age-related defects in CD4 T cell cognate helper function lead to reductions in humoral responses. *J Exp Med* 200:1613-1622.

Goidl, E.A., J.B. Innes, and M.E. Weksler. 1976. Immunological studies of aging. II. Loss of IgG and high avidity plaque-forming cells and increased suppressor cell activity in aging mice. *J Exp Med* 144:1037-1048.

Goronzy, J.J., and C.M. Weyand. 2013. Understanding immunosenescence to improve responses to vaccines. *Nature immunology* 14:428-436.

Haynes, L., S.M. Eaton, E.M. Burns, T.D. Randall, and S.L. Swain. 2003. CD4 T cell memory derived from young naive cells functions well into old age, but memory generated from aged naive cells functions poorly. *Proc Natl Acad Sci U S A* 100:15053-15058.

Haynes, L., P.J. Linton, S.M. Eaton, S.L. Tonkonogy, and S.L. Swain. 1999. Interleukin 2, but not other common gamma chain-binding cytokines, can reverse the defect in generation of CD4 effector T cells from naive T cells of aged mice. *J Exp Med* 190:1013-1024.

Jagger, A., Y. Shimojima, J.J. Goronzy, and C.M. Weyand. 2014. Regulatory T cells and the immune aging process: a mini-review. *Gerontology* 60:130-137.

Lages, C.S., I. Lewkowich, A. Sproles, M. Wills-Karp, and C. Chougnet. 2010. Partial restoration of T-cell function in aged mice by in vitro blockade of the PD-1/ PD-L1 pathway. *Aging cell* 9:785-798.

Linterman, M.A., W. Pierson, S.K. Lee, A. Kallies, S. Kawamoto, T.F. Rayner, M. Srivastava, D.P. Divekar, L. Beaton, J.J. Hogan, S. Fagarasan, A. Liston, K.G. Smith, and C.G. Vinuesa. 2011. Foxp3+ follicular regulatory T cells control the germinal center response. *Nat Med* 17:975-982.

Linton, P.J., and K. Dorshkind. 2004. Age-related changes in lymphocyte development and function. *Nature immunology* 5:133-139.

Miller, J.P., and D. Allman. 2003. The decline in B lymphopoiesis in aged mice reflects loss of very early B-lineage precursors. *J Immunol* 171:2326-2330.

Mirza, N., M.A. Duque, A.L. Dominguez, A.G. Schrum, H. Dong, and J. Lustgarten. 2010. B7-H1 expression on old CD8+ T cells negatively regulates the activation of immune responses in aged animals. *J Immunol* 184:5466-5474.

Nishioka, T., J. Shimizu, R. Iida, S. Yamazaki, and S. Sakaguchi. 2006. CD4+CD25+Foxp3+ T cells and CD4+CD25-Foxp3+ T cells in aged mice. *J Immunol* 176:6586-6593.

Nurieva, R.I., Y. Chung, G.J. Martinez, X.O. Yang, S. Tanaka, T.D. Matskevitch, Y.H. Wang, and C. Dong. 2009. Bcl6 mediates the development of T follicular helper cells. *Science* 325:1001-1005.

Phair, J., C.A. Kauffman, A. Bjornson, L. Adams, and C. Linnemann, Jr. 1978. Failure to respond to influenza vaccine in the aged: correlation with B-cell number and function. *The Journal of laboratory and clinical medicine* 92:822-828.

Raynor, J., C.S. Lages, H. Shehata, D.A. Hildeman, and C.A. Chougnet. 2012. Homeostasis and function of regulatory T cells in aging. *Curr Opin Immunol* 24:482-487.

Sage, P.T., L.M. Francisco, C.V. Carman, and A.H. Sharpe. 2013. The receptor PD-1 controls follicular regulatory T cells in the lymph nodes and blood. *Nature immunology* 14:152-161.

Sakaguchi, S., D.A. Vignali, A.Y. Rudensky, R.E. Niec, and H. Waldmann. 2013. The plasticity and stability of regulatory T cells. *Nat Rev Immunol* 13:461-467.

Sasaki, S., M. Sullivan, C.F. Narvaez, T.H. Holmes, D. Furman, N.Y. Zheng, M. Nishtala, J. Wrammert, K. Smith, J.A. James, C.L. Dekker, M.M. Davis, P.C. Wilson, H.B. Greenberg, and X.S. He. 2011. Limited efficacy of inactivated influenza vaccine in elderly individuals is associated with decreased production of vaccine-specific antibodies. *J Clin Invest* 121:3109-3119.

Scollay, R.G., E.C. Butcher, and I.L. Weissman. 1980. Thymus cell migration. Quantitative aspects of cellular traffic from the thymus to the periphery in mice. *Eur J Immunol* 10:210-218.

Shahinian, A., K. Pfeffer, K.P. Lee, T.M. Kundig, K. Kishihara, A. Wakeham, K. Kawai, P.S. Ohashi, C.B. Thompson, and T.W. Mak. 1993. Differential T cell costimulatory requirements in CD28-deficient mice. *Science* 261:609-612.

Shvarts, A., T.R. Brummelkamp, F. Scheeren, E. Koh, G.Q. Daley, H. Spits, and R. Bernards. 2002. A senescence rescue screen identifies BCL6 as an inhibitor of anti-proliferative p19(ARF)-p53 signaling. *Genes Dev* 16:681-686.

Tsuji, M., N. Komatsu, S. Kawamoto, K. Suzuki, O. Kanagawa, T. Honjo, S. Hori, and S. Fagarasan. 2009. Preferential generation of follicular B helper T cells from Foxp3+ T cells in gut Peyer's patches. *Science* 323:1488-1492.

Walford, R. 1969. The Immunologic Theory of Aging. *Munksgaard Press*

Williams, L.M., and A.Y. Rudensky. 2007. Maintenance of the Foxp3-dependent developmental program in mature regulatory T cells requires continued expression of Foxp3. *Nature immunology* 8:277-284.

Wollenberg, I., A. Agua-Doce, A. Hernandez, C. Almeida, V.G. Oliveira, J. Faro, and L. Graca. 2011. Regulation of the germinal center reaction by Foxp3+ follicular regulatory T cells. *J Immunol* 187:4553-4560.

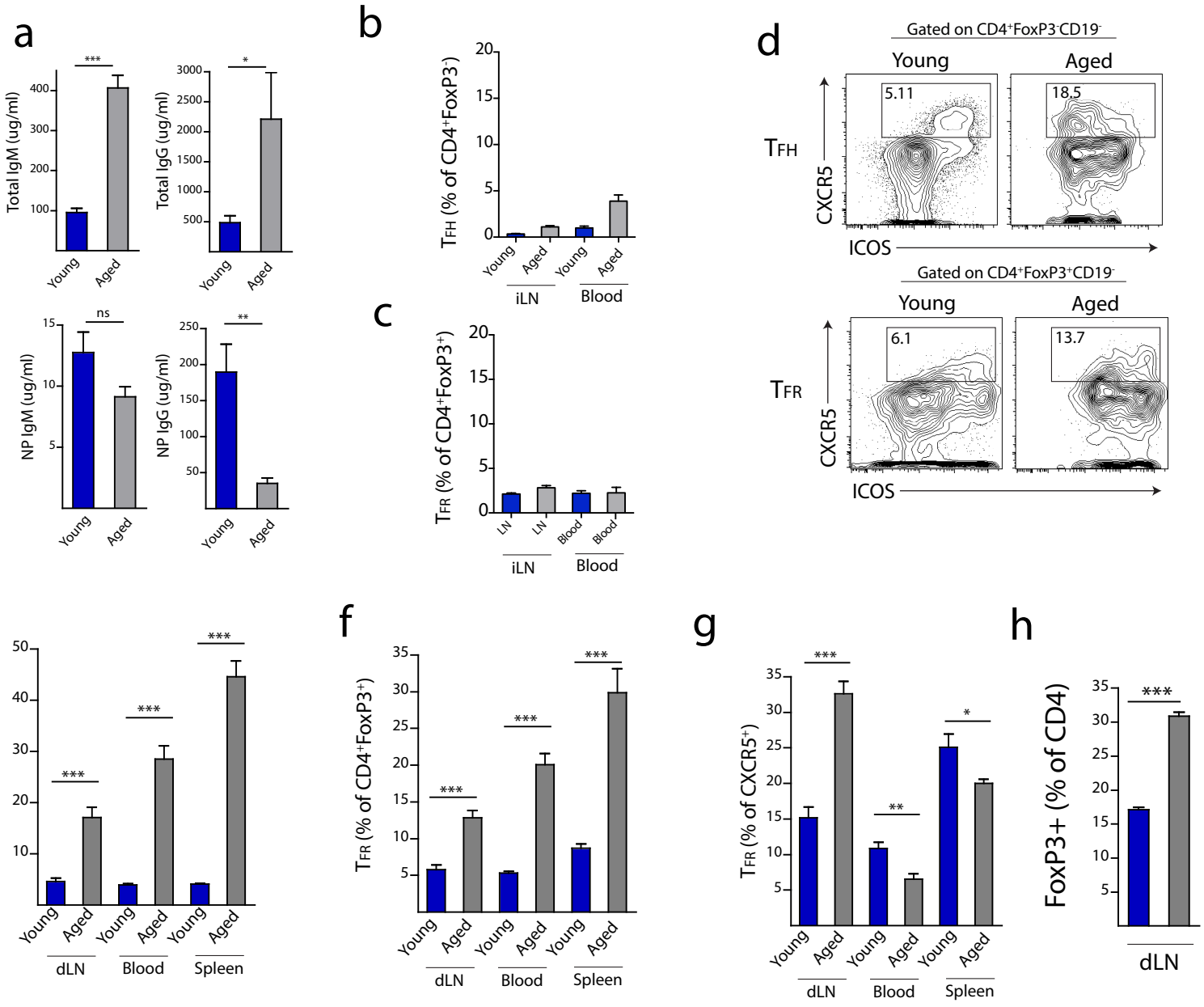

Sage Figure 1

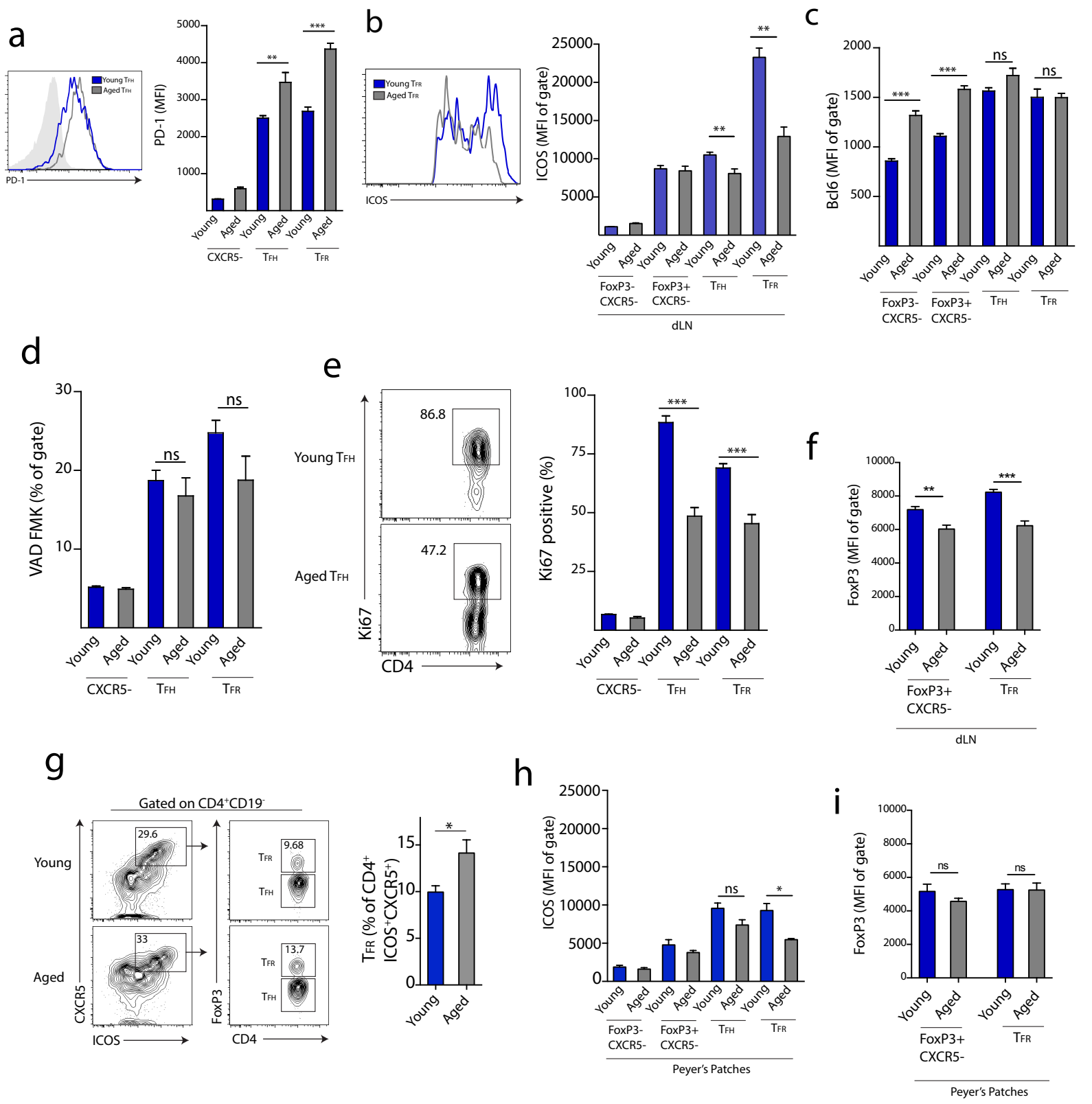

Sage Figure 2

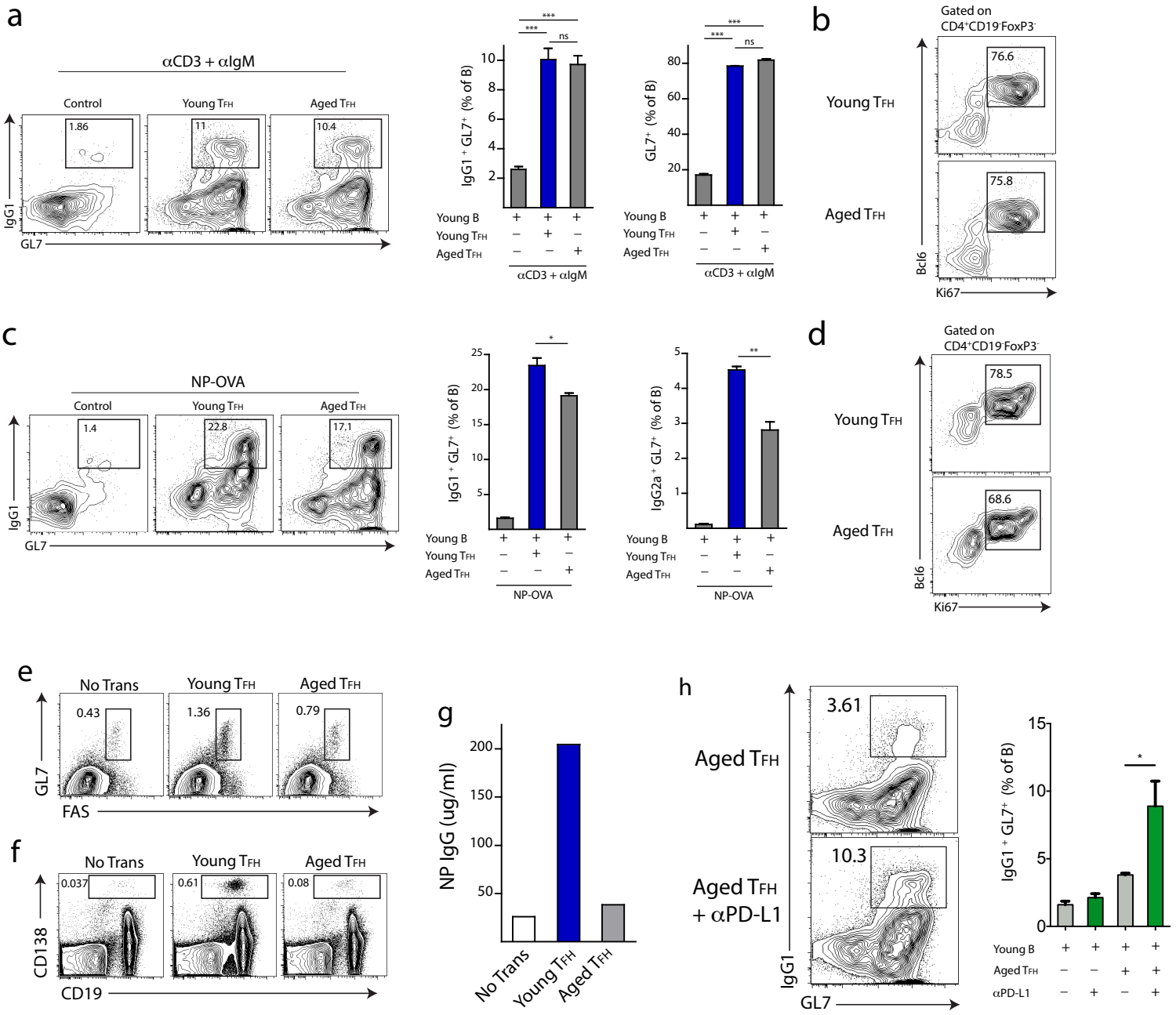

Sage Figure 3

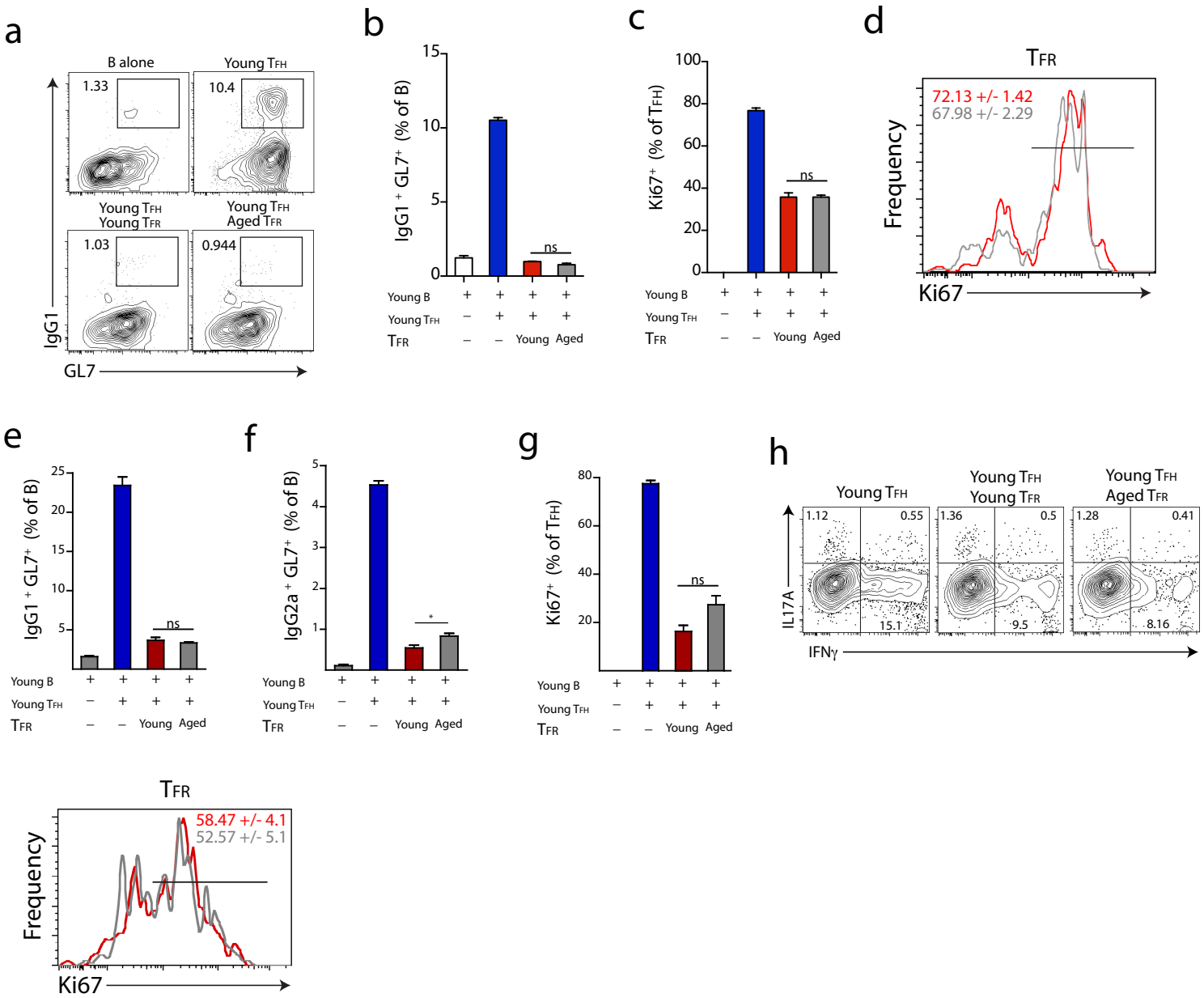

Sage Figure 4